

ELECTROMAGNETIC AND VIBRATION ENERGY HARVESTING UTILIZING A
PIEZOELECTRIC DEVICE

by

Misa Ngoc Vo

A thesis submitted to the faculty of
The University of North Carolina at Charlotte
in partial fulfillment of the requirements
for the degree of Master of Science in
Applied Energy and Electromechanical Systems

Charlotte

2015

Approved by:

Dr. Maciej A. Noras

Dr. Ryan S. Adams

Dr. Wesley Williams

©2015
Misa Ngoc Vo
ALL RIGHTS RESERVED

ABSTRACT

MISA NGOC VO. Electromagnetic and vibration energy harvesting utilizing a piezoelectric device. (Under the direction of DR. MACIEJ A. NORAS)

The main goal of this research is to design an energy harvesting device that produces enough power to supply a voltage sensor deployed on a power line. Energy harvesting using piezoelectric material is one of the promising methods of powering the sensor. The operating environment of the sensor is rich in electromagnetic fields and mechanical vibrations. Conversion of these unused energies into electricity can extend the sensor's battery life, or even eliminate the battery and associated maintenance. Therefore, maintenance safety hazards and operating cost of the sensors can be reduced. This research investigates a novel method of retrieving energy simultaneously from both electromagnetic fields and mechanical vibrations.

Two harvesters were arranged with three different physical layouts to examine their functionality and evaluate by output power density. The harvester with the layout exhibiting the highest power density was used to tune to the operating frequency (60 Hz) and examined for impedances loading effect. The harvesting system was then tested using electromagnetic fields created by a current carrying wire in combination with mechanical vibrations generated by a mechanical shaker. Data obtained in these tests were used to estimate power output in the real power line environment. The maximum recorded output power density was much higher than typical power density reported in the literature for piezoelectric energy harvesters [12]. According to the experimental data, ten harvesters should be able to produce enough power to supply the sensor in the operating environment.

ACKNOWLEDGMENTS

I would like to thank my adviser, Dr. Maciej A. Noras, for his guidance, support, and encouragement. Since I was undergraduate student, he has encouraged me to go above and beyond my perceived limits, and was always there whenever I ran into trouble. I would also like to thank my committee members, Dr. Wesley Williams and Dr. Ryan S. Adams for their interest and expertise in guiding my work, and answering my questions.

Special thanks to Mr. Green Franklin, Data Acquisition Technician of Mechanical Engineering and Engineering Science Department for always not only let me borrow equipment, but also for his availability and willingness to help me. Another special thanks to Dr. Peter L. Schmidt for his expertise, interest, and proofreading my work.

Grateful thanks to the UNC Charlotte Energy Production and Infrastructure Center Undergraduate Research Grant Committee for generous funding of the proof of concept project, which is part of this work, and to the UNCC Engineering Technology & Construction Management Department for providing me the opportunity and for supporting funds to complete this work.

Sincere thanks to my classmates, Brett Cockerham and Robert Garris for assisting me build a part of my testing setup; and to Benjamin Rhoades for proofreading this thesis.

Last but not least, many and many thanks to my family and friends for their support, motivation and tolerance that allowed me to accomplish this wonderful work.

TABLE OF CONTENTS

CHAPTER 1:	INTRODUCTION	1
CHAPTER 2:	LITERATURE REVIEW	3
2.1	General Overview of Energy Harvesting	3
2.1.1	Advantages of Energy Harvesting	3
2.2	Mechanical Vibration and Electromagnetic Fields Energy Harvesting – Overview	4
2.2.1	Mechanical Vibration Energy Harvesting	4
2.2.2	Electromagnetic Fields Harvesting	7
2.2.3	Hybrid Methods Combining Mechanical and Electromagnetic Harvesting	10
2.3	Theoretical Background	17
2.3.1	Mechanical Energy Harvesting	17
2.3.1.1	Beam Vibration Theory - Natural Frequency	17
2.3.1.2	Stiffness of Material/Young’s Modulus of Elasticity	19
2.3.1.3	Longitudinal Versus Tensile Mode	19
2.3.1.4	Rectangular Beam vs Trapezoidal Beam	21
2.3.2	Electromagnetics Energy Harvesting	21
2.3.2.1	Electromagnetic Fields Surrounding a Conductor	21
2.3.2.2	Electromagnetic Fields of a Magnet	22
2.3.3	Hybrid Methods	23
2.3.4	Characteristic of Operating Environment	24
2.4	Proposed Approach: Simultaneous Harvesting from Electromagnetic Fields and Mechanical Vibrations	24

	vi
2.4.1 Proof of Concept [3]	25
2.4.2 Proposed Ideas for Improvement	26
2.4.2.1 Use of D31 and D33 Simultaneously	26
2.4.2.2 Flexible Materials	26
2.4.2.3 Modular Design	27
2.4.3 Advantages and Challenges	27
CHAPTER 3: METHODOLOGY	28
3.1 Proof of Concept Experiment Set up	28
3.2 Physical Layout Setup	30
3.3 Experimental Testing and Setup	32
3.3.1 Experimental Setup	33
3.3.2 Mechanical Vibration Measurement	35
3.3.2.1 Influence of Vibration Magnitude	35
3.3.2.2 Influence of Vibration Frequency	36
3.3.3 Electromagnetic Fields Measurement	36
3.3.3.1 Investigation on Current	36
3.3.3.2 Investigation of Resonant Frequency	36
3.3.3.3 Investigation of the Distance between the Harvester and the Wire	37
3.3.4 Theoretical Modeling Method	39
3.3.5 D33 Versus D31 Coupling	39
3.3.6 Harvester 2 with Physical Layout IIIB Further Investigation	40
3.3.6.1 Influence of Measuring Equipment and Loading	40
3.3.6.2 Electrical Impedance Resonance Influence	41

3.3.6.3 Combinations of Electromagnetic Fields and Mechanical Vibration	41
CHAPTER 4: RESULTS	43
4.1 Proof of Concept Experiment [3]	43
4.1.1 Experimental Results	43
4.1.2 Modeling Results	44
4.1.3 Modular Design Test	45
4.2 High Modulus of Elasticity Materials	46
4.2.1 Cantilever Beam with Distributed Magnets - Physical layout I Results	47
4.2.1.1 Mechanical Vibration Test	47
4.2.1.2 Electromagnetic Field Test	49
4.2.1.3 COMSOL Multiphysics Simulation	51
4.2.1.4 Effect of Distance (EMF Test Only)	52
4.2.1.5 D33 versus D31 Coupling	54
4.2.2 Cantilever Beam with Magnets at Free End - Physical Layout II Results	56
4.2.2.1 Mechanical Vibration and EMF Frequency Varying	56
4.2.3 Increasing Magnetic Fields Interactions – Physical Layout III	59
4.2.4 Harvester 2 Impedance Problem	67
4.2.5 Electrical Impedance Resonance Influence	69
4.2.6 Sources Combination Test	73
4.2.7 Prediction for Power Line Environment	75
CHAPTER 5: CONCLUSIONS	79
5.1 Discussion	79
5.2 Possible Future Work	83

	viii
BIBLIOGRAPHY	84
APPENDIX A: SOURCES COMBINATION THEORETICAL CALCULATION MATLAB CODE	88
APPENDIX A: OUTPUT POWER PREDICTION ON OPERATING ENVIROMENT MATLAB CODE	89

CHAPTER 1: INTRODUCTION

Recent advances in the development of portable devices have led to the need for small, wireless, and portable power supplies. One of the promising methods of providing this type of a power source is energy harvesting. Energy harvesting systems used in production of electricity have been shown to provide clean operation (no pollution) and overall power stability. There are many different sources of energy that can be harvested; however, the primary source for energy harvesting is from kinetic energy [1]. Kinetic energy harvesting is typically in the form of displacement which can be used to generate electrical power. There are three approaches to convert this displacement into electricity: magnetic induction, electrostatic energy recovery, and use of piezoelectric materials [2]. Among these three methods, piezoelectric materials are known for their robustness, simple structure, ease of fabrication, and low cost.

The main goal of this research is to design an energy harvesting device that produces enough power to supply a voltage sensor deployed on a power transmission line [3]. The sensor at the existing stage of development requires 130 mW for operation. The environment in which the sensor operates has an abundance of electromagnetic energy from the power line and kinetic energy from mechanical vibrations. Conversion of that energy into electricity that powers the sensor can prolong the sensor's battery life, or even eliminate the need for the battery and the need for maintenance. That, in turn, provides cost savings and reduces safety hazards to the maintenance personnel. In this

research a novel method of retrieving energy simultaneously from both electromagnetic fields (EMF) and mechanical vibrations is investigated. The experiments are assisted by modeling of developed harvesters and their topologies, in order to provide information that allows for optimization of the device.

Previous research by the author included development of an energy harvesting device consisting of a piezoelectric material inserted between two permanent magnets [4]. A working prototype of the energy harvesting device, capable of harvesting energy from an EMF and mechanical vibration, was demonstrated [4]. Nevertheless, due to the materials used (low flexibility ceramics) and the construction of the harvester, the device did not produce the expected amount of output power. This research served as a proof of concept of combining magnets and piezoelectric materials to harvest EMF and vibrations. Based on these preliminary results, investigations focused on piezoelectric materials with higher flexibility. These harvesters were assembled in three different physical structures and examined. Output power density for all design cases was measured and a harvester with the highest output power density was used to evaluate impedance effect, tuned to 60 Hz (operating frequency of the power line), and then evaluated in the laboratory conditions using available ENF and vibration sources. Based on the test data the power output was estimated for operation in a real power line environment.

CHAPTER 2: LITERATURE REVIEW

2.1 General Overview of Energy Harvesting

Energy harvesting is a viable source of clean and renewable energy that appears increasingly popular at this time of debates on the effect of global warming [2]. It is a process of converting energy in a form of heat, light, vibration, and movement available in the environment to a more convenient and useful form such as electricity [5]. Energy harvesting devices vary from large-scale (utilizing solar, wind, thermal, geothermal, biomass, and hydrogen energy) to small-scale power devices that can take advantage of additional set of physical, chemical and bio-phenomena, including EMF, pyro-, thermo- and piezoelectricity, fuel cells, enzymatic sugar conversion, etc. [2]. In this work, the focus is on low power density harvesting from mechanical vibrations and EMF, as these two energy forms are readily available in the power line surroundings.

2.1.1 Advantages of Energy Harvesting

Even though the power requirements for electronic devices are decreasing as they become more energy efficient, a battery is still their main power source. Batteries have to be recharged or replaced, and proper disposal and recycling of batteries is a global challenge [5] [6]. They are also bulky and heavy, especially when compared to microelectronic devices that they supply with power [7]. A typical battery has a short life span that is not practical for devices, which are expected to last more than 10 years [8]. In addition, some of the electronics can be located in difficult to reach areas: embedded in

people or animals, installed inside structures (bridges, roads, buildings), placed on satellite systems, etc. Energy harvesting has a potential to become a solution that can provide power in these applications [9].

2.2 Mechanical Vibration and Electromagnetic Fields Energy Harvesting – Overview

2.2.1 Mechanical Vibration Energy Harvesting

Energy harvesting from mechanical vibrations involves three main approaches: magnetic induction, electrostatic energy recovery, and use of a piezoelectric material. Induction approaches (typically used in electromagnetic harvesters) utilize Faraday's law for creation of an electric potential due to variable magnetic field. In harvesting devices it usually takes form of a permanent magnet that, due to mechanical excitation, moves in close proximity to a potential-inducing coil. Such generators can utilize linear or circular motion of the magnet [5]. Electrostatic harvester devices utilize the varying capacitance of two vibrating conductors to produce electricity [10]. Piezoelectric generators are devices that convert mechanical vibration, in the form of stress or strain on piezoelectric material, into electrical energy. The main component of a piezoelectric generator is a piezoelectric material which is capable of converting mechanical energy to electrical energy and vice versa [11].

Performance of energy harvesting devices is usually assessed by evaluating the power density value. Power density is the ratio of output power to volume. Reported typical power density of piezoelectric generators is about $200 \mu\text{W}/\text{cm}^3$ [12]. In comparison, electrostatic harvesters can produce power density within the range of $50\text{-}100 \mu\text{W}/\text{cm}^3$ and electromagnetic harvesters are capable of less than $1 \mu\text{W}/\text{cm}^3$ [12]. Based on these power density values, piezoelectric generators have the power advantage

over the other two techniques. In addition, they have been known for their robust, adaptable and simple structure, and are also easy to fabricate [13]. Piezoelectric devices can be considered a relatively mature technology, as they have already been broadly utilized as power sources in sensing, telemetry, and MEMS applications [2]. In the past, researchers have proposed the use of piezoelectric materials to harvest human motion for example in wearable and implantable electronics [14],[15]. Piezoelectric generators are also used in applications that take advantage of fluid flow [16], oscillation [17], mechanical vibration and interaction of multiple sources of vibrations and of magnetic fields [1]. Among all of these methods of using piezoelectric devices to retrieve energy, most of the designs proposed harvest only one source of energy.

The discussion in the following sections presents applications of piezoelectric materials in different types of harvesting.

Numbers of studies have been conducted that provide information on energy harvesting from humans using wearable and implantable electronics [5]. One example, as presented by Shenck and Paradiso [14], is to use piezoelectric elements in shoes, positioned in the back (heel) and front portion of an insole. The back element was made of a push button like-type multilayer piezoelectric. The front element was a piezoelectric layer combined with metal layer. As a result, 1.3 mW and 8.4 mW of power were produced with a 250 k Ω and 500 k Ω load respectively.

Another example is collecting energy from a human's wrist motion [15]. The device uses a frame of free moving masses with piezoelectric cantilevers at the end of the frame. According to the authors, the power density theoretically obtained by this device was up to 40 $\mu\text{W}/\text{cm}^3$. Electric signals retrieved through a piezoelectric due to human

motion usually have a high amplitude and low frequency which requires the size of the harvester to be comparatively large [5].

A piezoelectric harvester utilizes most vibration and oscillation forms of environmental energies [5]. For example, they can take advantage of a fluid flow: a piezoelectric strip placed under the ocean is used, to supply power to the sensors installed on floating buoys [16]. In oscillating applications, a piezoelectric material has been added as a part of a motor's rotor as well as attaching a device to a windmill blade [17]. The author claimed the theoretical possible output power density was 100 W/cm^3 . The maximum measured output power density was 91 W/cm^3 at the resonance frequency of 1000 Hz.

The most researched piezoelectric structure in harvesting is a cantilever beam [13]. Use of different beam shapes, such as triangular, trapezoidal, and rectangular has been shown to have a significant effect on power output capability [18]. One example of using a cantilever beam is a research project reported by Yeon et al. [19]. A cantilever beam was processed with a combination of different layers such as a thin film lead zirconate titanate piezoelectric, a membrane layer, a diffusion barrier layer (ZrO_2), silicon layer and with an optional added mass. The size of the harvester beam was $170 \mu\text{m} \times 260 \mu\text{m}$. The piezoelectric beam had a proof mass at the free end and was designed for a given range of resonant frequencies. The output power was found to be 0.74 mW/cm^3 . The research team also claimed that this device could be comparable to lithium ion batteries. This work supports the theory that a cantilever beam is an efficient structure for mechanical vibration energy harvesting.

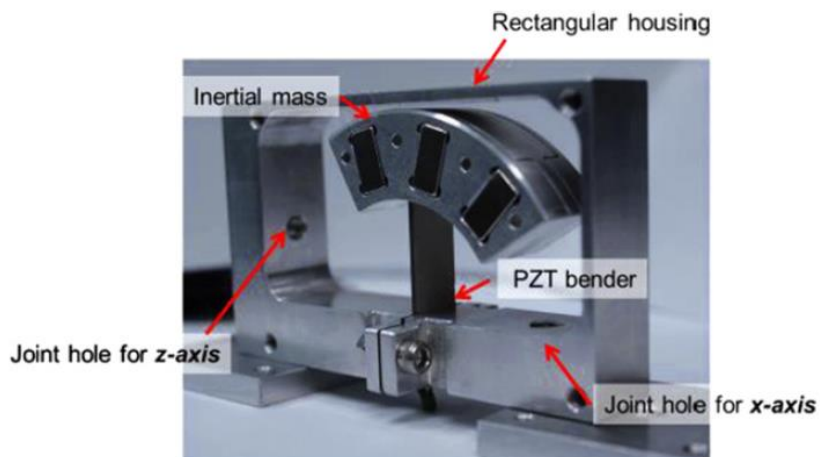


Figure 1: Asymmetric proof mass piezoelectric cantilever beam design [19]

In order to improve the piezoelectric beam performance, a proof mass can be added to the free end of the piezoelectric cantilever [7]. An experiment utilizing an asymmetric proof mass was reported by Jong C. Park and Jea Y. Park [20]. The devices consist of a piezoelectric bimorph beam with the volume of 36 x 10 x 0.72 mm and an asymmetric proof mass shown in Figure 1. This proof mass allowed the harvester to vibrate and gather energy in two dimensions. As a result, output power was 7.5 mW harvested when vibration was applied horizontally and 1.4 mW with vertically vibration applied.

2.2.2 Electromagnetic Fields Harvesting

There are multiple ways of harvesting power from electromagnetic sources. They all can be categorized into three groups: resonant, rotational, and hybrid methods [5]. Resonant generators often contain a permanent magnet as a moving mass associating with a coil. Most resonant generators function in a low frequency and have low output power densities. Most of them require the use of a spring, which reacts to the external vibration force. The first electromagnetic resonant generator for a small scale application

was proposed in 1995 by Williams [21]. The design schematic is shown in Figure 2a below. Later in 2000, the design was built; it contained an upper mass-spring on a substrate and a lower pick-up coil substrate as shown in Figure 2b [22]. This device produced lower electrical power than expected due to the nonlinear effects of spring stiffening.

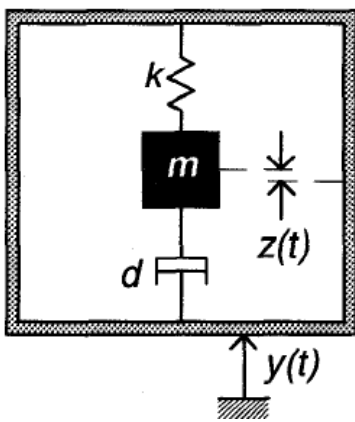


Figure 2a: Diagram of linear inertia generator [21]

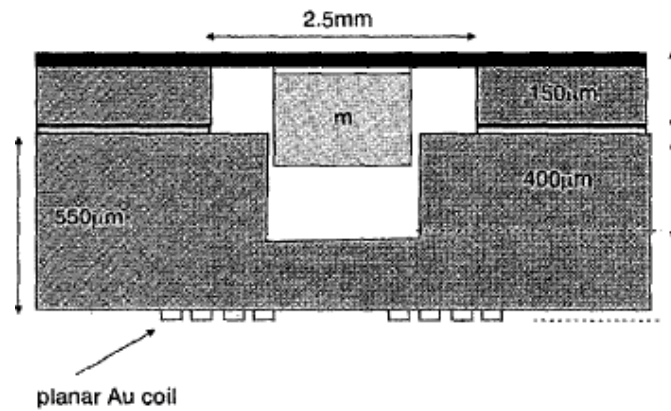


Figure 2b: Williams's resonant generator [22]

Rotational generators depend on a rotational mechanical energy [5]. In comparison with resonant generator, they operate at high rotational speeds and frequencies. An example of an electromagnetic rotational device is an axial-flow micro-turbine power generation system designed and built by Holmes and his team [23]. The device consist of a polymer rotor with diameter of 7.5 mm, embedded with permanent magnet in between two silicon stators as shown in Figure 3 below. The harvester produced an output power of 1.1 mW at a 30000 rpm rotational speed. One disadvantage

of this rotational electromagnetic generator is the complexity of the design. For instance, the design of Holmes required silicon micromachining and laser etching [5].

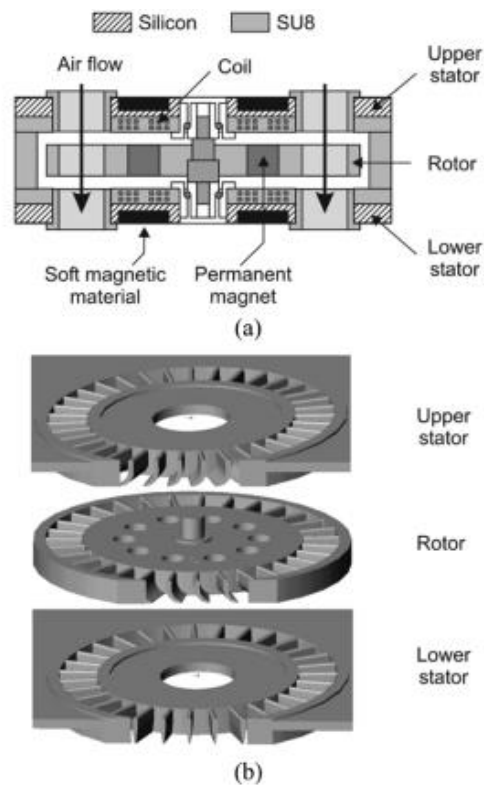


Figure 3: Holmes' and his team's rotational generator [23]

A hybrid generator is a combination of resonant generator and rotational generator, and it is implemented using an imbalanced rotor. Kayakawa and Seiko Company introduced a hybrid generator to harvest energy from human movement for wrist watches [5]. Since these types of electromagnetic generators rely on the use of magnets, one of the disadvantages of these generators is calibrating them for maximum efficiency due to variable properties of magnets and restriction on the number of coil turns. This hybrid also generates a small vibrational amplitude.

2.2.3 Hybrid Methods Combining Mechanical and Electromagnetic Harvesting

Both electromagnetic generators and piezoelectric generators are suitable for producing power in the microwatt to mW range. Several researchers successfully tried to use these types of piezoelectric devices in EMF energy harvesting. As stated earlier, mechanical vibrations come from mechanical excitations of structures, earthquakes, operation of motors and machinery, and other types of vibrational energy. However, they can also be produced by interaction of magnetic forces with the main focus on low frequencies (up to the third harmonic of 60 Hz).

It is well known that an AC current in a conductor generates a magnetic field. If this field interacts with any other magnetic field, for example that of a permanent magnet, the resulting mechanical vibration can be scavenged. A piezoelectric transducer design of Leland et al. demonstrated use of this concept by utilizing vibration from the interaction of a magnet and an AC power cord [24]. The device consists of a piezoelectric bimorph cantilever beam with two magnets acting as a moving mass as shown in Figure 4. The piezoelectric beam was mounted to custom-machined aluminum brackets. This structure vibrated when the magnet was placed on top of a conducting AC wire, which generated voltage. Subsequently, the output power was 208 μW and 345 μW with 9 A_{RMS} and 13 A_{RMS} of AC current respectively.

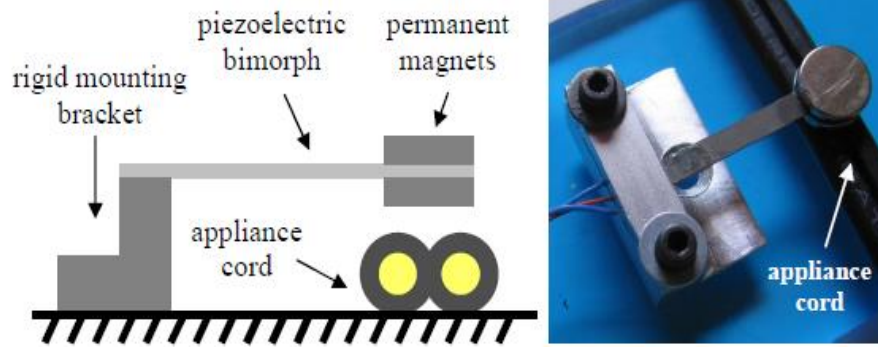


Figure 4: Leland's piezoelectric harvester design [24]

Another example of gathering vibration energy using magnets and magnetic fields is a self-powered wireless sensor node for the power line monitoring from Xu et al. [25] [26]. The harvester consists of multiples layer of piezoelectrics cantilever beam with multiple magnets as added mass as shown in Figure 5. The sensor was mounted on top of a power line wire. A stopper frame was used to protect the harvester from breaking in the case of high current such as lightning strike. The research team claimed that output power generated $100 \mu\text{W}$ to 1 mW when the current increased from 30 A to 142 A [25]. Later, they also reported maximum output power was 2.7 mW from a 20 A current [26].

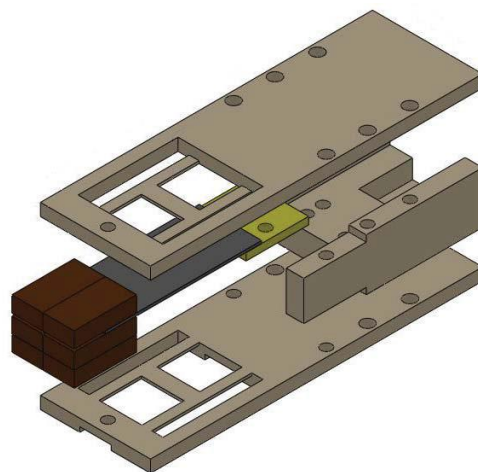


Figure 5: Xu's electromechanical harvester [26]

He et al. has investigated a similar concept [27]. The device, shown in Figure 6, used a piezoelectric cantilever beam. The beam consisted of two layers of piezoelectrics, beryllium bronze and a piezoelectric P-51. At the free end of the beam a combination of magnets and a mass were attached. To enhance the magnetic flux density three rectangular Neodymium (NdFeB) magnets were used. The first magnet (M1) was placed horizontally while the other two magnets (M2 and M3) were placed vertically at both ends of the first magnet to act as a support structure (Magnetic Yoke in Figure 6). An energized AC wire was placed in the center of the space surrounded by three magnets. The harvester generated 1.58 mW under a 216 k Ω load resistor with a 50 Hz resonant frequency of 6 A_{RMS} current.

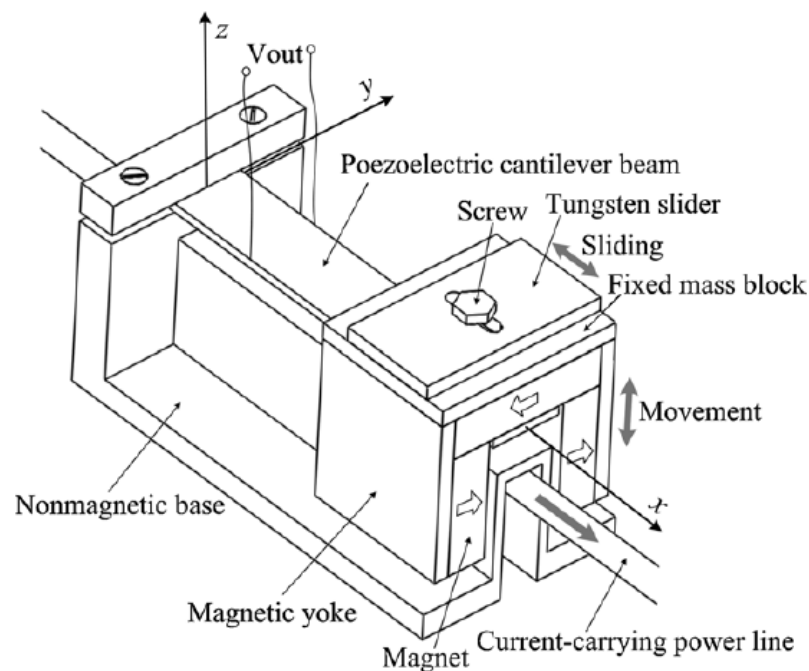


Figure 6: Magnetic circuit design [27]

A similar method of generating vibration from a combination of a permanent magnet and an AC magnetic field was developed by Uzun and Kurt [28]. The device was made of a piezoelectric beam with a ferromagnetic mass attached at the free end. The beam was clamped vertically (pendulum type configuration) and placed near an electromagnet as shown in Figure 7. The electromagnet generated a magnetic field, and attraction and repelling forces acted on a ferromagnetic mass. This made the beam move and produced voltage. As a result, an average power of $79 \mu\text{W}$ was collected.

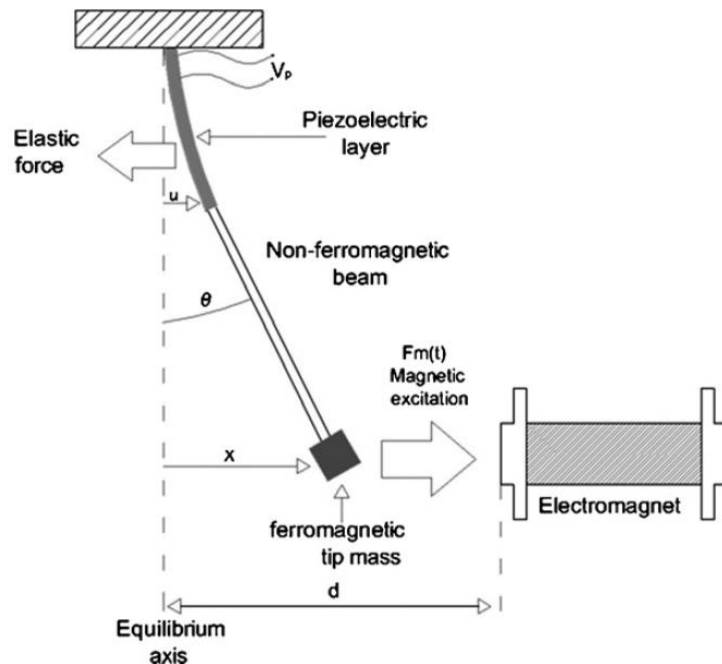


Figure 7: Uzun's and Kurt's piezoelectric design [28]

Another similar harvester structure was studied by Ferrari et al. [29]. The harvester was composed of a piezoelectric material printed on a stainless steel cantilever beam [29]. A permanent magnet with vertical magnetization facing the free end was used to increase the deflection of the beam and at the same time created a bistability as shown

in Figure 8. The authors reported an increase of about 400% compared with the linear case, but did not report any power values.

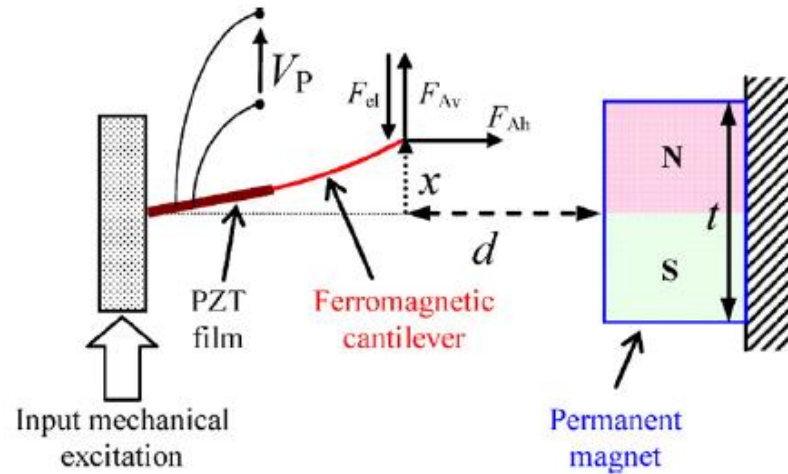


Figure 8: Ferrari's harvester design [29]

Another design called the “multipurpose piezoelectric” energy harvester was proposed by Fan et al. [30]. The harvester consisted of a frame, a ferromagnetic material roller, a piezoelectric patch mounted on a metal layer and a magnetic added mass at the end as shown in Figure 9. They claimed that the harvester was capable of retrieving energy from sway and multi-directional vibration. In sway motion, the roller sensed the motion and moved toward the added mass. The magnetic interaction between the roller and the added mass pulled the harvester up, and released when the roller was moved backward. The cantilever beam was used to harvest multi-directional vibration. The research was performed and reported at a proof of concept stage and no output power value was provided.

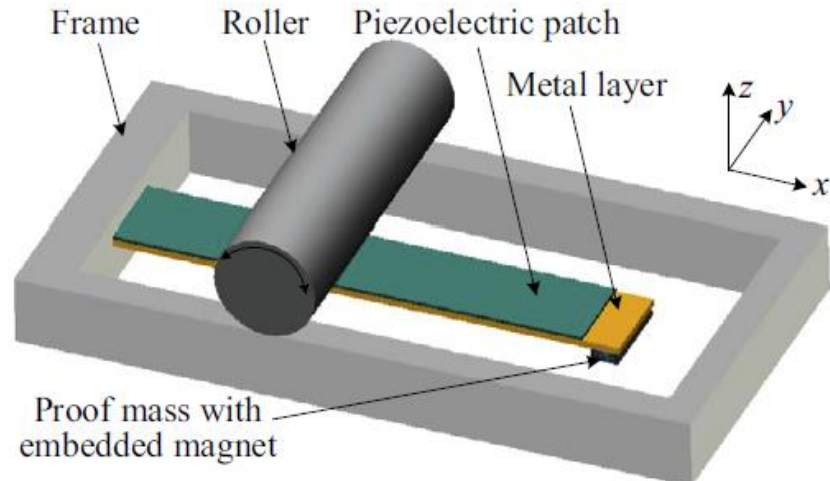


Figure 9: Multipurpose piezoelectric energy harvester [30]

Challa et al. presented a “coupled piezoelectric–electromagnetic” energy harvester [31]. The harvester included a piezoelectric cantilever beam with a permanent magnet attached at the free end as shown in Figure 10. A coil was used to couple the electromagnetic damping and piezoelectric damping together. Experiments were conducted with two different piezoelectric materials, a strip actuator and a fiber composite. As a result, output power of the coupled device was $332 \mu\text{W}$ and $182 \mu\text{W}$ for strip actuator and fiber composite respectively. An increase in the total output power of 30% and 65.5% was claimed (for the strip actuator and fiber composite respectively) compared to the stand alone piezoelectric generator.

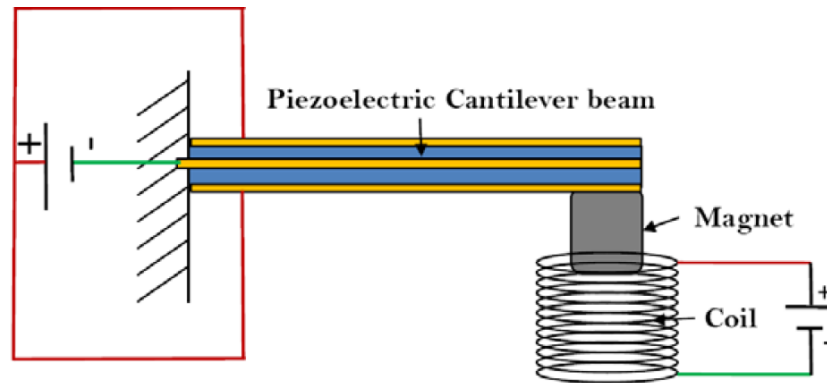


Figure 10: Coupled piezoelectric – electromagnetic energy harvester [31]

As mentioned earlier, the output power density value is often used to assess the harvester design or suitability for an application. Table 1 presents the output power density values of the device described in this section. Overall, the cantilever beam design was one of the most effective ways to harvest mechanical vibration. The output power density depends on modulus of elasticity of materials used, length of the beam, and added mass. Many researchers have used magnets as added mass. Using a magnet is also one way to generate magnetic field interaction (between magnets or between magnets and current carrying wire) which converts EMF energy to mechanical vibration. Interaction between magnets and current appears to have the highest power density, since the magnetic field of the wire can be increased by increasing the current going through of the wire. Most energy harvesters were focused on harvesting one source of energy. It would be advantageous to build a piezoelectric generator to convert more than one source of energy.

Table 1: Literature review summary (included harvesters with obtainable data only)

Researchers	Piezoelectric Size (mm)	Output Power (mW)	Power Density (mW/cm ³)
V. Hugo Schmidt	-	-	9100
Yoen et al.	-	-	0.74
Jong C. Park and Jea Y. Park	36 x 10 x 0.72	7.5	28.94
	36 x 10 x 0.72	1.4	5.40
Leland et al.	31.8 x 3.2 x 0.38	0.345	8.92
Xu et al.	28.57 × 12.7	2.7	7.44
He et al.	25 x 6 x 0.35 and 25 x 6 x 0.42	1.58	13.68
Uzun and Kurt	70 x 32 x 1.5	0.079	0.02
Challa et al.	36 x 20 x 0.16	0.332	2.88

2.3 Theoretical Background

The following sections discuss the theoretical background supporting energy harvesting including beam vibration theory, Young's modulus of elasticity, piezoelectric operating modes and electromagnetic behaviors of magnets and conductors, and their interaction.

2.3.1 Mechanical Energy Harvesting

2.3.1.1 Beam Vibration Theory - Natural Frequency

Vibrations are the oscillation, or shaking of a mechanical system about an equilibrium position [32]. They are present when there is an external, time-varying force acting on an object. Vibration is present in almost every physical system [34]. Since vibrations exist in most environments, there is a tremendous amount of available energy that can be harvested.

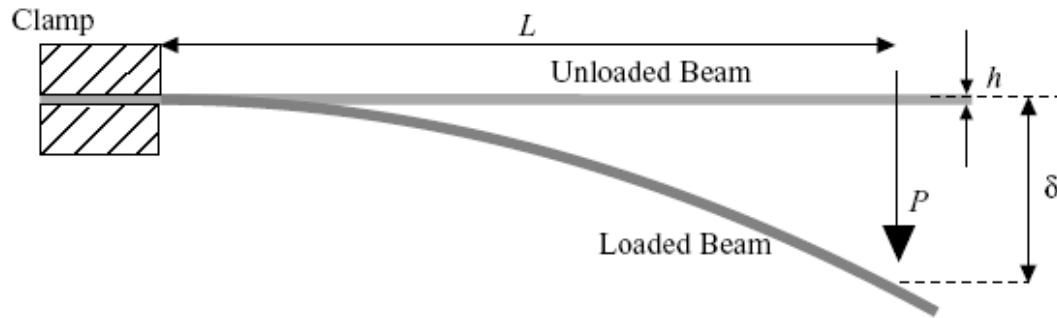


Figure 11: Cantilever beam with point load at free end [34]

Since the proposed harvester utilizes a cantilever beam configuration to harvest mechanical vibration, it is best to understand the effect of natural frequency and deflection of this beam. A cantilever beam is the most popular structure used in vibration harvesting. Cantilever beams for this application usually come in a rectangular cross-section configuration. Under an external impulse, this beam will deflect or vibrate. This vibration is described as its natural frequency. There are different modes of vibrations. For simplicity, let's consider a simple case of a cantilever beam with a point mass load at the edge of the free end as shown in Figure 11. The maximum deflection, Δ , is shown in Equation (1) [35] below.

$$\Delta = \frac{PL^3}{3EI} \quad (1)$$

Where: P = mass

L = effective length (distance between clamping and mass load, can be different with the actual length of harvester)

E = modulus of elasticity

I = area moment of inertia of a rectangular cross section

The fundamental natural frequency of the cantilever beam is described in Equation (2):

$$\omega_n = \sqrt{\frac{3EI}{mL^3}} \quad (2)$$

Different natural frequencies yield different deflection. From Equation (1) and (2) [35], it can be concluded that the lower the vibration mode, the higher the deflection. In other words, the first vibration mode has the highest deflection. By selecting the physical properties and size of the beam, the desirable deflected shape (or higher output power) can be obtained.

2.3.1.2 Stiffness of Material/Young's Modulus of Elasticity

When a piezoelectric material is driven by a vibrating force, it produces an electric field at the same vibrating frequency as the force. The vibration frequency in the atmosphere usually ranges from 50-250 Hz [12]. This means that the piezoelectric energy harvester must have a natural frequency within this range for maximum output power. As stated above, a lower natural frequency will result in a higher deflection, which produces maximum output voltage in a piezoelectric cantilever beam. Based on equation (2), the deflection also depends on the material's modulus of elasticity. The modulus of elasticity is the ratio of stress to strain [34]. A low modulus of elasticity indicates that the material is flexible and yields a higher deflection. Therefore, low elasticity materials (or flexible materials) could be preferably considered to achieve a higher output power out of a harvester.

2.3.1.3 Longitudinal Versus Tensile Mode

The piezoelectric coefficients that affect the output power are charge constant (d), voltage constant (g), and coupling factor (k). The charge constant, is the ratio of

polarization over stress [37]. This coefficient conveys how suitable a piezoelectric material is for use in a strain application. The voltage constant conveys how much electric field is generated when a mechanical stress is applied. The electromechanical coupling factor signifies the effectiveness when converting mechanical energy to electrical energy [12].

There are three operating modes for piezoelectrics, -33, -31, and -15 as shown in Figure 12. In the mode -33 (longitudinal mode), the applied force is the same as the electrical polling direction as shown in Figure 3a. In mode -31 (tensile mode), the applied force is perpendicular to the polling direction (Figure 12b). Mode -15 (shear mode), has two identical applied forces on each opposite face of the piezoelectric element parallel with polling direction (Figure 12b). Even though there are three operating modes, only longitudinal and tensile modes are practical for energy harvesting [10], due to how the external force is applied to the piezoelectric material. Although the tensile mode is the most commonly used, the magnetic coupling factor is higher in the longitudinal mode. Sodano [10] also concluded that in a small force and low vibration environment, a piezoelectric cantilever beam utilized in tensile mode is more efficient than longitudinal mode. In contrast, a piezoelectric cantilever beam used in longitudinal operating mode produces more energy under high vibration [10].

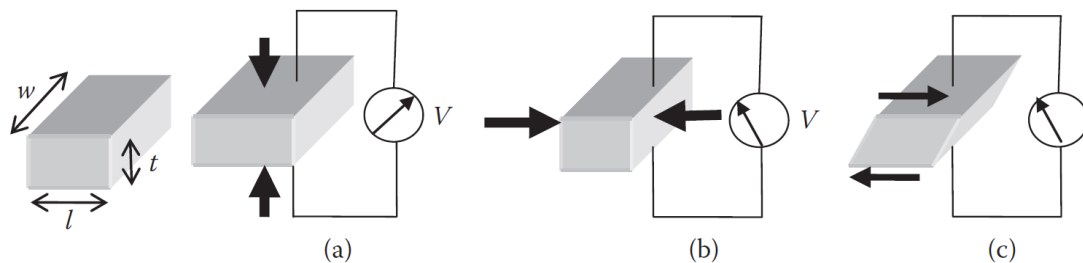


Figure 12: Operating modes [12]

2.3.1.4 Rectangular Beam vs Trapezoidal Beam

According to Anton and Sodano [10], a rectangular cantilever beam has been most commonly used for piezoelectric energy harvesting. In a piezoelectric material, electrical energy output is proportional to the amount of strain input [38]. Maximum output power is collected when the harvester beam is strained at its limit before it breaks and distributed uniformly along the surface of the beam. For a cantilever beam, the stress is maximum at the fixed end, which means that the strain is maximum at the fixed end which implies that a portion of the piezoelectric material is unused. In order to improve the efficiency, use of triangular or a trapezoidal shape was considered. In theory it may provide an increase in the output power by 50%, however experiments have shown only a 30% increase [38].

2.3.2 Electromagnetics Energy Harvesting

2.3.2.1 Electromagnetic Fields Surrounding a Conductor

According to Ampere's Law, any electric current creates a magnetic field. For a long straight wire, a magnetic field surrounds the wire as shown in Figure 13.

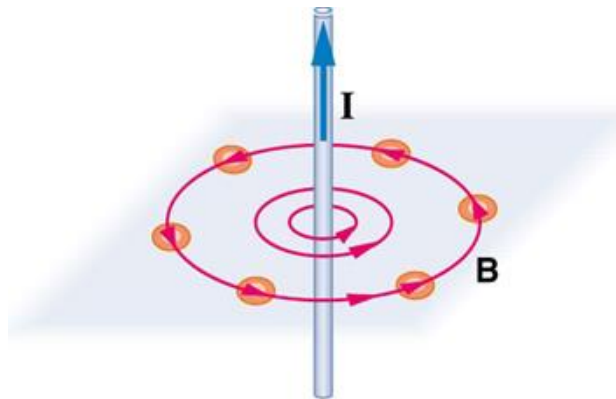


Figure 13: Magnetic field of a straight wire [39]

The current (I) will generate a magnetic field (B) in a direction shown in Figure 13. Also, the B field is stronger when it is close to the wire. Equation (3) below describes the relationship between the B field and the current at any given point of interest. In this equation, i is a current, μ_0 is the permeability of free space and r is the radial-distance from origin to the point of interest. A resulting magnetic force is shown in Equation (4) where L is the effective length.

$$\vec{B} = \frac{\mu_0 i}{2\pi r^2} \quad (3)$$

$$\vec{F} = \vec{i} L \times \vec{B} \quad (4)$$

2.3.2.2 Electromagnetic Fields of a Magnet

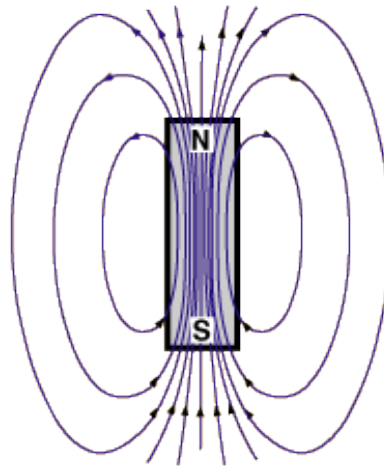


Figure 14: Magnetic field of a bar magnet [40]

A permanent magnet creates a fixed magnetic field. When the magnet is placed close to a current conducting wire, the magnetic field of the magnet and the wire will interact with each other which can cause an attracting or repelling force. This force's magnitude depends on the overlap length on the plane that contains both the magnet and

wire. Based on Equation (4), this force also depends on the magnetic field intensity of the magnet, current of the wire and geometric arrangement of both these elements. By carefully selecting a magnet's orientation and placement with respect to the wire, maximum force can be achieved. For example, as shown in Figure 15, assume the same current and magnet, higher effective length is achieved by having horizontal placement of the magnet (Figure 15a) rather than a vertical orientation.

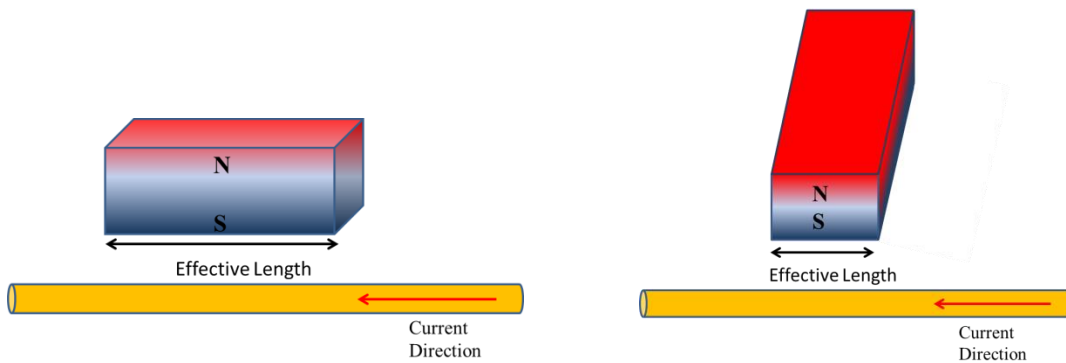


Figure 15a: Magnets and wire arrangement

1

Figure 15b: Magnets and wire arrangement

2

2.3.3 Hybrid Methods

Since both a wire conducting current and a permanent magnet generate magnetic fields, placing a magnet close to a wire conducting current can generate attraction or repelling forces. If the wire is conducting alternating current (AC), the induced forces on the magnet change from attraction to repelling since the magnetic field generated by AC in a conductor is constantly changing. As a result, a mechanical vibration is produced. If the magnet is attached to one end of the piezoelectric cantilever beam, the magnetic fields interaction causes the beam to deflect, hence producing power as shown in Figure 16.

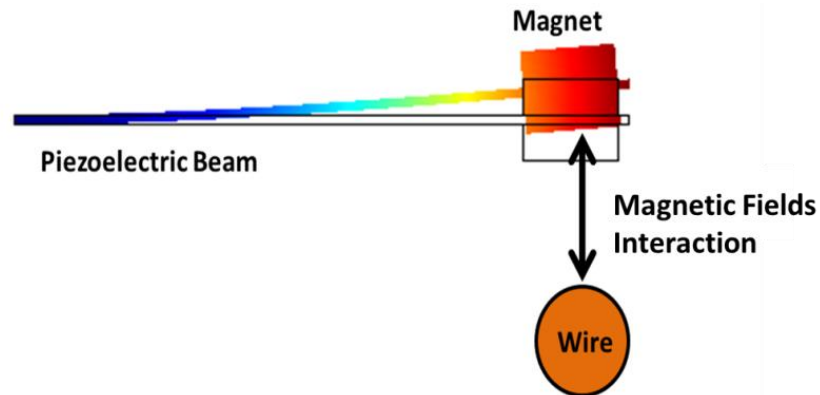


Figure 16: Magnetic fields interactions produce a deflection on a piezoelectric cantilever beam

2.3.4 Characteristic of Operating Environment

As mentioned, the operating environment of the harvester is within a power line environment. There are three types of wind vibrations in the power line, Aeolian, galloping and wake induced [44]. Among the three type, Aeolian have the widest frequency range from 3 Hz to 150 Hz. Frequency range for galloping is 0.08 to 3 Hz and 0.15 to 10 Hz. Amplitude of the vibration depends on conductor diameter and range between a factor 0.01 to 1 of conductor diameter. A typical distribution line uses a 500 kcmil conductor carrying maximum current of 100 to 600 A [45].

2.4 Proposed Approach: Simultaneous Harvesting from Electromagnetic Fields and Mechanical Vibrations

For energy harvesting in the power line environment it would be advantageous to build a device which is able to simultaneously convert mechanical vibrations and EMF into electricity. The proposed EMF and vibration harvester device is comprised of a piezoelectric beam with different permanent magnet arrangements as an added mass and

as a way to increase magnetic fields interaction. As, shown in Figure 16 when the harvester is placed in an EMF, the magnets exert mechanical force and bend the piezoelectric material. In addition, any other types of mechanical movement in the harvester's vicinity, such as building vibrations or machine vibration, can provide an additional stress on the harvester cantilever, thus producing electricity. Based on the preliminary results and other harvesters' design, the output power density of each single harvester may be small (in mW range). For this reason, modular design was investigated in the proof of concept. With this option, power output can be scaled in a form of plug-in modules, which will allow for the output power of the harvester to be adjusted.

2.4.1 Proof of Concept [3]

Preliminary experiment was conducted to examine the concept on harvesting EMF. Experimental details of this proof of concept are in the Result Section. The highest output of a single harvester assembly was about $0.1 \mu\text{W}$ while three modular harvesters connected together yielded about $0.34 \mu\text{W}$. There is no observable deflection since the magnets and the piezoelectric are relatively thick and stiff. The whole assembly was held together only by magnetic attraction force between the magnets. While the power output of the harvester is very small, it is important to keep in mind that this structure is not optimized at all, and serves only as a proof of concept.

A model using COMSOL Multiphysics with the same conditions as the preliminary experiment was also created. The modeled output voltage magnitude was about $13 \text{ mV}_{\text{p-p}}$, which was higher than the experimental results ($1.12 \text{ mV}_{\text{p-p}}$). Both voltages have the same shape and frequency. The magnitude difference comes from imperfections of the physical assembly of the harvester such as air gaps between the

magnets and piezoelectric materials and the assembly's fixed end mounting geometry. A higher output voltage, and therefore, output power can be expected with an appropriate design of the physical assembly.

2.4.2 Proposed Ideas for Improvement

2.4.2.1 Use of D31 and D33 Simultaneously

As described earlier, the two main operating modes of a piezoelectric material are the 31 and 33 mode. The 33 mode has a higher coupling coefficient than the 31 mode. However, the 31 mode is more commonly used. By having the harvester operate in both the 33 and 31 modes simultaneously should produce increased output power.

2.4.2.2 Flexible Materials

The most daunting challenge for the proposed optimization of the design is to identify ways to increase the output power. The research plan is to find more efficient materials, to design a better way to physically connect the piezoelectric and magnetic materials, and to develop a proper testing system. In previous research [3], due to the materials used (low flexibility materials) and the construction of the harvester, the model did not produce any significant amount of output power.

Based on Equations (1) and (2), deflection of a cantilever beam partially depends on a modulus the elasticity of the beam materials. By utilizing materials with decreased Young's modulus and determining a more efficient physical layout for the harvester, the output power could increase enough to supply the power line sensor. Flexible materials introduced into the design and tuning to the highest energy source allow higher deflection of the harvester at resonance frequency. Also, arranging the magnets in optimized configuration could result in higher magnetic field interaction forces, which then will

produce higher power output. If these improvements are successful, the proposed energy harvesting device can serve as an auxiliary power source for portable electronic devices.

2.4.2.3 Modular Design

As stated earlier, the main goal of this harvester is to supply power to the power line sensor. The sensor used as a basis of design is still in the development process with a power requirement subject to change. Modular design gives an option of flexible harvester capacity for scalable output power. The harvester modules can be combined in parallel for increased output power. Earlier testing has proved that this harvester's modular design option is viable.

2.4.3 Advantages and Challenges

The main goal for this proposed optimized device is to harvest enough energy to power the power line sensor. However, this device could be used to power many other types of sensors due to its efficient performance. Also, this harvester's cost is low and it could serve as a backup power source because it could generate extra usable electrical power for many types of small devices. Furthermore, this device could extend a battery's life.

Challenges may arise in constructing the harvester, mainly due to adhesives requires to connect the piezoelectric and the harvester so that the forces from magnets are sufficiently transferred. Other challenges may be experienced while testing for energy harvesting using specific sources of energy. Undesirable vibration such as building vibrations, machine vibration and vibration from human walking, exists which could affect the test results under both mechanical vibration and EMF.

CHAPTER 3: METHODOLOGY

The preliminary results demonstrated a working concept. The proposed ideas for improvement suggested using elastic materials and finding the best physical arrangement for maximum output power. For all testing, output power density was the main assessment criteria for different physical layouts. Two different harvesters and three physical layouts were studied. The optimal location of the harvester in proximity with the wire, harvester behavior under changing vibration magnitude and electromagnetic current, and frequency responses were investigated. A COMSOL model was also used in conjunction with the experiment to verify the results. The harvester with the highest output power density was then used for an impedance study, tuning for 60 Hz, source combination and output power prediction in the operating environment.

3.1 Proof of Concept Experiment Set up

The purpose of this test is to ensure that the concept on harvesting EMF produces the predicted behavior. A series of experiments were conducted. During these experiments, an APC 850 piezoelectric material, poled in the d33 mode with electrodes on the surfaces and two NdFeB magnets (K&J Magnetics) were used. Two types of magnets, magnetized through thickness (BX082-N52) and through the width of the magnet plate (B82X0), were tested. The advantage of using these materials for the harvester is the ease to build (no adhesive required), and simple structure. The test setup is shown in Figure 17.

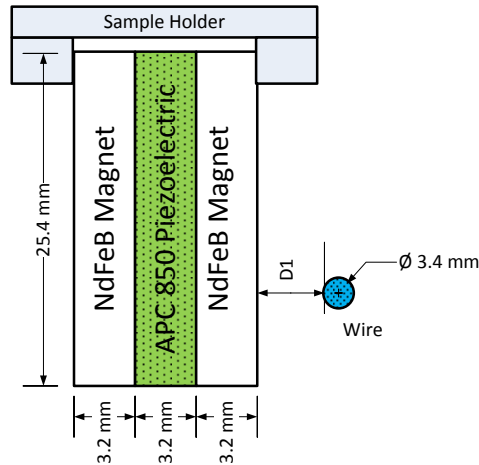


Figure 17a: Side view of the proof of concept harvester

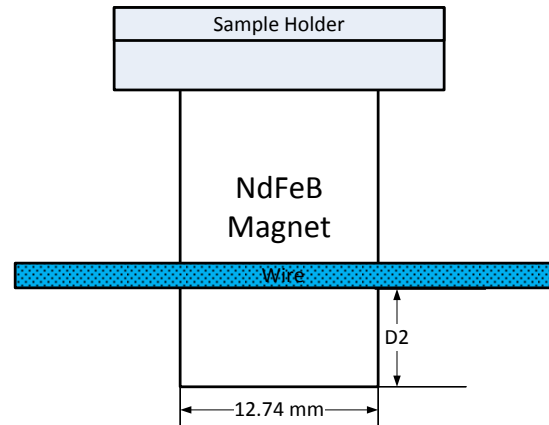


Figure 17b: Front view of the proof of concept harvester

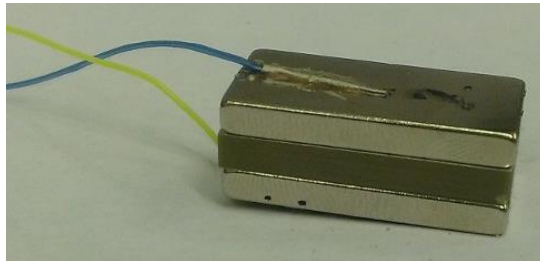


Figure 17c: Photo of the proof of concept harvester

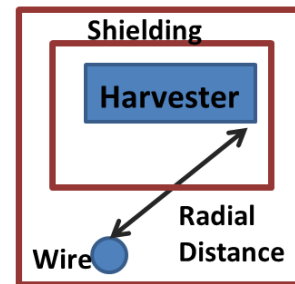


Figure 17d: Harvester with shielding

The piezoelectric material was inserted between two magnets and placed in proximity with a wire conducting 6 A_{RMS} of 60 Hz AC current (Figure 17a and 17b). As the magnetic field generated by the current interacts with the magnets, the resulting force is transferred to the piezoelectric material, causing a stress on this material and generating electric potential on the electrodes. To make sure that there was no capacitive coupling between the wire and the piezoelectric, the harvester structure was shielded from the wire and the surroundings with a grounded aluminum foil as shown in Figure 17d. In this way, there is no electric field influences on the piezoelectric material electrodes. Radial

distance was defined as the distance between the wire and the harvester (shown in Figure 17). The output voltage was measured with shield and without shield.

Modular design capability was also tested for this proof of concept. In the experiment, each of the harvesters was placed closest to the AC wire and measured the output power. Then, these harvesters were combined in parallel configuration. The test was completed with a single harvester, a set of two harvesters and a set of three harvesters. The theoretical output power levels were calculated by the total power of each harvester while the experimental powers were the measured power with the harvesters in parallel. The experimental and theoretical results were compared and concluded the harvester was capable of modular design. Although, this harvester was capable of modular design, the output power was still small. This signified the use of flexible magnets was a viable option.

3.2 Physical Layout Setup

This section describes all physical layouts for with the proposed ideas for improvement. There are three physical layouts used. The main purpose of testing multiple physical layouts was to find for the physical layout that generated the highest output power density. Two different harvesters, named Harvester 1 and Harvester 2, were used for all the physical layouts. Harvester 1 consisted of a single Smart Material MFC M-8541-P2 piezoelectric deposited on a polycarbonate sheet as shown in Figure 40, top harvester. Harvester 2 is a commercial Mide Vulture V21BL that is composed of two piezoelectric layers as shown in Figure 40, bottom harvester. The size of Harvester 1 was larger than Harvester 2 (displaced in Figure 18b and 18c).

Table 2 presents computer sketches of all physical layouts for Harvester 1 and 2. Physical layout I consisted of three set of magnets, two magnet A and one magnet B, placed on top and bottom of the harvester as shown in column 2 of Table 2. The magnetic interaction would be increased by using multiple set of magnets. This configuration also allowed the harvesters to have more squeezing interaction due to multiple magnets used. Conversely, physical layout II only had one set of magnet (magnet C) placed at the free end of the harvesters as displaced in column 3 of Table 2. This physical layout allowed the harvester to have more deflection. The main different between physical layout II and III was magnet A added at the bottom magnet C. For physical layout III, this magnet A has two different orientations with respected to the wire used to generate EMF energy source, perpendicular (physical layout IIIA) and parallel (physical layout IIIB). These physical layout IIIA and IIIB represented the situation described in Figure 15a and 15b which the magnetic field interaction was higher due to an increasing in effective length by placing the magnet parallel to the wire. The tests for all physic layouts are described in the next section.

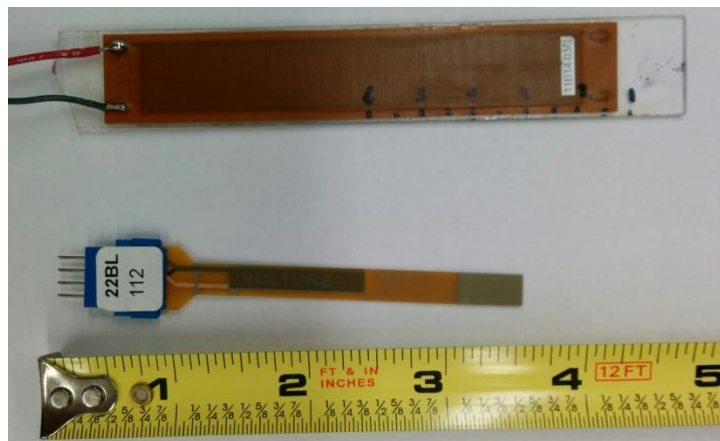


Figure 18a: Physical image of Harvester 1 and 2

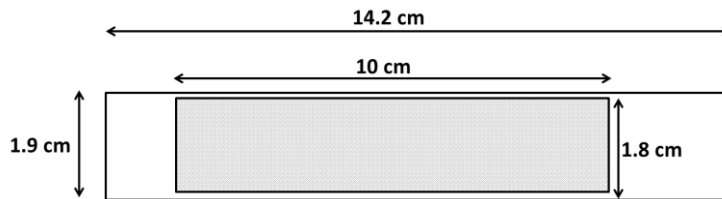


Figure 18b: Harvester 1 Computer Sketch

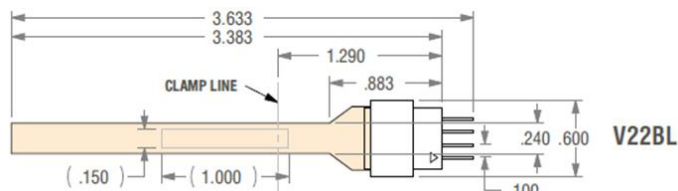


Figure 18c: Harvester 2 Computer Sketch (Measurements are in inches) [43]

Table 2: Physical layouts sketch summary

	Harvester 1	Harvester 2
Physical layout I		
Physical layout II		
Physical layout III A		
Physical layout III B		

3.3 Experimental Testing and Setup

There were two main parts of the experiment test, mechanical vibration, and EMF. For both mechanical vibration and EMF, output power responses under various input magnitude and current were examined. The optimal distance with respect to the wire was studied for EMF. Output power response under various input magnitude and

distance test was only performed for the first physical layout since the output power would show the same behavior for all physical layouts. All physical layouts were examined to determine the natural frequency and output power for each harvester. A simulation model was built to ensure the experiment results under EMF for all physical layouts. Harvester with the physical layout produced the highest power were then used for further test, including impedance study, tune to 60 Hz, sources combination and prediction for operating environment.

3.3.1 Experimental Setup

A fixture was designed to hold the harvester in place to test for EMF and mechanical vibration as shown in Figure 19. In addition to the holder, vibration generation devices used for the mechanical testing portion includes a shaker, waveform generator and amplifier as shown in Figure 20. For all of the tests, an output of the harvester was connected to a resistor load and output power was calculated as shown in Equation (5).

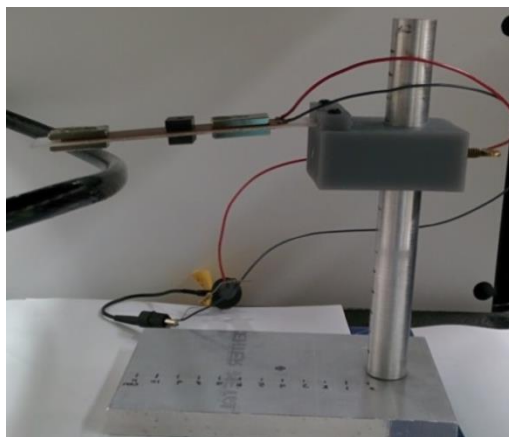


Figure 19a: Photo of the assembly

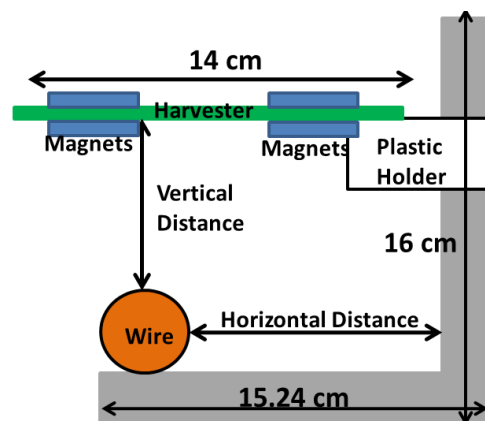


Figure 19b: Piezoelectric beam holder assembly

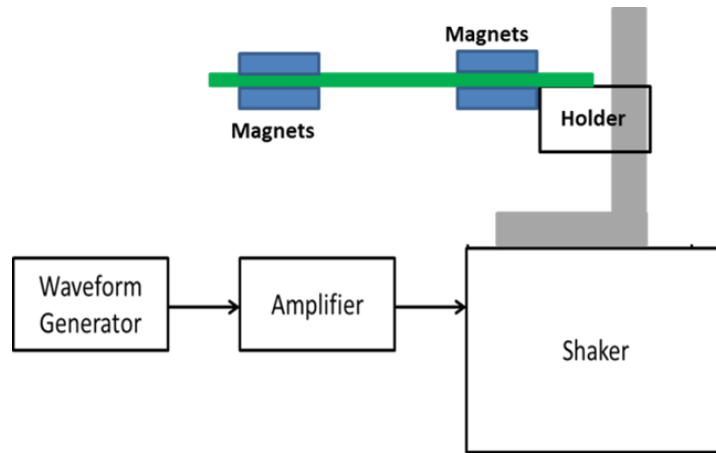


Figure 20: Experimental set up

$$P = \frac{V_{RMS}^2}{R} \quad (5)$$

Table 3a shows the piezoelectric material constants and other parameters for the harvester beams used. Different physical configurations, length of the beam and added mass, were tested to verify the simulated model and tuned for 60 Hz frequency. Table 3b below presents materials, components and equipment used.

Table 3a: Harvesters' parameters

	Constant	Value	Unit
Proof of Concept (Ceramic Piezo)	d13	175	10^{-12} C/N
	d33	400	10^{-12} C/N
	E	0.054	GPa
Harvester 1 (MFC Smart Material)	d13	400	pC/N
	d33	-170	pC/N
	E	30.336	GPa
Harvester 2 (Vulture Mide)	d13	390	10^{-12} C/N
	d33	-190	10^{-12} C/N
	E	Not Given	

Table 3b: Equipment and components used

Testing	Equipment/Components	Model
Proof of Concept	Piezoelectric	Ceramic APC 850
	Magnets	J&K Magnets: <ul style="list-style-type: none"> • B82X0: 1/2 x 1/8 x 1 inches thick • BX081-N52: 1 x 1/2 x 1/16 inches thick • BX082-N52: 1 x 1/2 x 1/8 inches thick
	Wire	Insulated 16 AWG
	Current Generator - Adjustable Isolation Transformer	POWER STAT Variable Transformer 146
	Load Resistor	10 k Ω to 10 M Ω
	Materials	Piezoelectric-Harvester 1
Plastic Cantilever Beam		Lexan 10 x 8 inches polycarbonate sheet
Piezoelectric-Harvester 2		Volture Mide V21BL
Resistor Loads		440 k Ω to 1 M Ω
Electromagnetic Fields	Wire	Insulated 1/0
	Current Generator	Kepeco BOP 6-125MG
Mechanical Vibration	Function Generator	Rigol DG 1022
	Amplifier	Brüel & Kjær Power Amplifier Type 2718
	Shaker	Brüel & Kjær Exciter Type 4809
Measuring Equipment	Oscilloscope	Rigol DS1052
	Probe	Tektronix P3010

3.3.2 Mechanical Vibration Measurement

3.3.2.1 Influence of Vibration Magnitude

In this experiment, a shaker was used to produce vibrations. This shaker required a waveform generator and amplifier input as displayed in Figure 20. The input voltage waveform generator controlled vibrations generated by controlling the current output of the amplifier. This current then regulated a displacement of the shaker. The input frequency was kept constant at 60 Hz and displacement was changed from 0.037 mm to 1.45 mm.

3.3.2.2 Influence of Vibration Frequency

The main purpose of this testing is to determine the natural frequency of the harvester. This measured natural frequency of the actual harvester is different from the calculated and simulation values due to physical construction and tolerance of the E coefficient. Also, material damping and mounting of the harvester could result in a slightly different value of natural frequency. For this test, the shaker displacement was kept at 0.147 mm and the input frequency was changed from 1 Hz to 440 Hz to search for the resonant frequencies.

3.3.3 Electromagnetic Fields Measurement

3.3.3.1 Investigation on Current

For this testing, both the wire and the wire's position will be fixed since in the real operating environment the harvester will be mounted in a fixed position. The vertical distance was 2.5cm and the wire was placed under the magnet at the end of the harvester's beam. The only changing parameter was current. Current amplitude varied from 3.535 to 88.375 A_{RMS} with a 3.535 A_{RMS} increment; input frequency was 60 Hz.

3.3.3.2 Investigation of Resonant Frequency

As discussed earlier, maximum power will be obtained when the resonance of the harvester beam matches the operating frequency of the powerline (60 Hz in the United States). The purpose of this test is to determine the natural resonance of the harvester. For this test, the same position as the investigation on current test was used. The input current amplitude was kept constant at 35.35 A_{RMS} . The frequency was varied from 10 Hz to 443 Hz to find the resonances, and the output voltage data were recorded.

3.3.3.3 Investigation of the Distance between the Harvester and the Wire

In the testing of EMF harvesting, the two independent parameters are the current flow in the wire and the distance between the wire and harvester. A fixture is designed to help hold the harvester and the wire for testing which is illustrated in Figure 17, also shown in the top part of Figure 18. To investigate the effect of the distance, the input current was $17.675 A_{RMS}$ at 60 Hz frequency. The origin was defined at a position where the cylindrical pole and the base of the holder met. Vertical distance was defined as the distance from bottom of harvester to the wire and horizontal distance was the distance from the fixture to the wire. Vertical distance was varied from 0 cm to 14 cm while horizontal distance was varied from 0 cm to 20 cm; an increment of 1cm was used for both distances. In the vertical position, the vertical distance was offset by 1.38 mm to ensure the harvester did not touch the wire when vibrating. The output was connected across a $1 M\Omega$ resistor.

A summary of experiment procedures used to find the highest physical layout and optimal location of harvester in regard to the wire are shown in Table 4.

Table 4: Experiment procedures summary

	Input	Setup
Mechanical Vibration- Amplitude Test	Frequency: 60 Hz	Same with EMF-Current Test
	Displacement: 0.037 to 1.45 mm	
Mechanical Vibration- Frequency Test	Sweep frequency from 1 Hz to 440 Hz to find peaks	Same with EMF-Current Test
	Displacement: 0.147 mm	
EMF-Current Test	Frequency: 60 Hz	The wire was under the free end magnets. Vertical distance was 2.5 cm
	Current amplitude: 3.535 to 88.375 A_{RMS} (3.535 A_{RMS} increment)	
EMF-Frequency Test	Sweep frequency from 1 Hz to 440 Hz to find peaks	Same with EMF-Current Test
	Current amplitude 35.35 A_{RMS}	
EMF-Horizontal Position Test (physical layout I only)	Frequency: 60 Hz	Origin: at cross section of the cylinder piece and the base. Vertical distance: 1 cm
	Current amplitude: 17.675 A_{RMS}	
	Horizontal Distance: 0 to 20 cm (1 cm increment)	
EMF-Vertical Position Test (physical layout I only)	Frequency: 60 Hz	Offset of 1.38 mm used to make sure the harvester does not touch the wire when vibrating. The wire was placed under the free end magnets
	Current amplitude: 17.675 A_{RMS}	
	Vertical Distance: 0 to 14 cm (1 cm increment)	

3.3.4 Theoretical Modeling Method

A COMSOL model was built to verify experimental results. The model was used to predict the influence of flexible materials, finding the most efficient physical layout and arrangement for the harvester. As discussed in the literature review, the harvester is built as a cantilever beam. The deflection of this beam depends on the mass, length, cross section geometry and the modulus of elasticity of the beam. Output power could be maximized when the natural frequency is close to 60 Hz, since the EMF is at 60 Hz. A modulus of elasticity (E) of magnets and piezoelectric elements was input into the model for each of these materials. In the proof of concept, a 3D model consisted of a Piezoelectric Devices Physics and Electromagnetic Physics were built. The Electromagnetic Physics calculated the resulting magnetic fields forces. This force was then used in the Piezoelectric Devices Physics as a load body to deflect the piezoelectric beam and generate output voltage. Instead of using the Electromagnetic Physics, a 2D model with Equation (4) used as a body load in Piezoelectric Devices Physic was use for the low E piezoelectric materials. This reduced the complexity and simulation time of the model.

3.3.5 D33 Versus D31 Coupling

The purpose of this test was to see the influence of piezoelectric operating mode. Since Harvester 2 was composed of two piezoelectrics embedded in layers of materials, the squeezing force of the magnet was not strong enough to produce measurable effect. For this reason, only Harvester 1 was used for this test. As mentioned, due to the large squeezing action since there were multiple magnets used, physical layout I would be the best layout to determine the effect of D33 versus D31. To test material in D33 mode, all

the edges of the harvester were fixed. The only action left would be squeezing in this case; hence, D33 mode. The frequency was kept at 60 Hz and current was adjusted from 35 to 88 A_{RMS} . When the harvester was at fixed on one side (like all experiments for elastic materials), the mechanical action under EMF source included squeezing and deflecting. Therefore, for D31, the output voltage was the subtraction of the fixed one side output voltage to the D33 case.

3.3.6 Harvester 2 with Physical Layout IIIB Further Investigation

As mention at the beginning of this section, the harvester and physical layout with the highest output power density was used to study for impedance of the system (including measurement equipment), tune to 60 Hz, sources combination and prediction. Harvester 2 with physical layout IIIB was the harvester that produced the highest output power density. This section describes the rest of the test procedures for Harvester 2 with physical layout IIIB.

3.3.6.1 Influence of Measuring Equipment and Loading

For all experiments, a resistive load was used and a voltage across this load was measured. Since a piezoelectric harvester produces a low power output, the resistive loading within a range of $k\Omega$ to $M\Omega$ was used. However, the load resistance, probe and oscilloscope resistance were close to that order of magnitude. These resistances of the scope and probe became a part of the load and generated more power loss.

Investigation on output voltage with resistor load of 10 $k\Omega$ to 10 $M\Omega$ was assessed. Depending on loading resistance, a correction factor may be used. As mention earlier, Harvester 2 consisted of two piezoelectrics both series and parallel connection of Harvester 2 was examined while in all other experiment, the two piezoelectrics of

Harvester were connected in series. Output voltages were measured for series and parallel connection with a probe reading of 10X and 1X. By switching between 10X and 1X reading, the impedance of the probe was changed from 1 M Ω to 10 M Ω . Since the impedance of the whole energy system depends on frequency and the harvester was designed to work at resonance, the resonance frequency of 37 Hz for parallel and 36 Hz for series connection was used.

Aside from the probe's and oscilloscope's resistances problem, according to the maximum transfer power condition, the loading resistor should be equal with a Thevenin Equivalent internal resistance of the piezoelectric. A simple equivalent circuit model of a piezoelectric material consists of a series resistance and capacitance [42]. The same result from the investigation of scope's and probe's impedance was examined to find the loading for maximizing transferred power.

3.3.6.2 Electrical Impedance Resonance Influence

To ensure that the electrical impedance of the harvester and the measurement equipment did not have influence of the measured output power, the impedance of the harvester and the measuring equipment were studied. An equivalent impedance model was built using Pspice with the measured impedance for Harvester 1 and 2. The frequency response was examined to ensure the resonance from electrical impedances was further from the natural frequencies of Harvester 1 and 2.

3.3.6.3 Combinations of Electromagnetic Fields and Mechanical Vibration

One of the goals of this research is to harvest multiple sources of energy, mechanical vibration and EMF. Therefore, the harvester was placed under conditions where both EMF and mechanical vibration were present. The purpose of this test is to see

whether there would be higher output power when both sources of energy are present.

The output voltage response of the Harvester 2 under mechanical vibration magnitude and current magnitude were obtained to predict for the operating environment.

CHAPTER 4: RESULTS

4.1 Proof of Concept Experiment [3]

This section describes the preliminary testing performed on the ceramic piezoelectric and served as a proof of concept EMF harvesting test. This proof of concept includes the experimental testing, modeling results, and modular design test.

4.1.1 Experimental Results

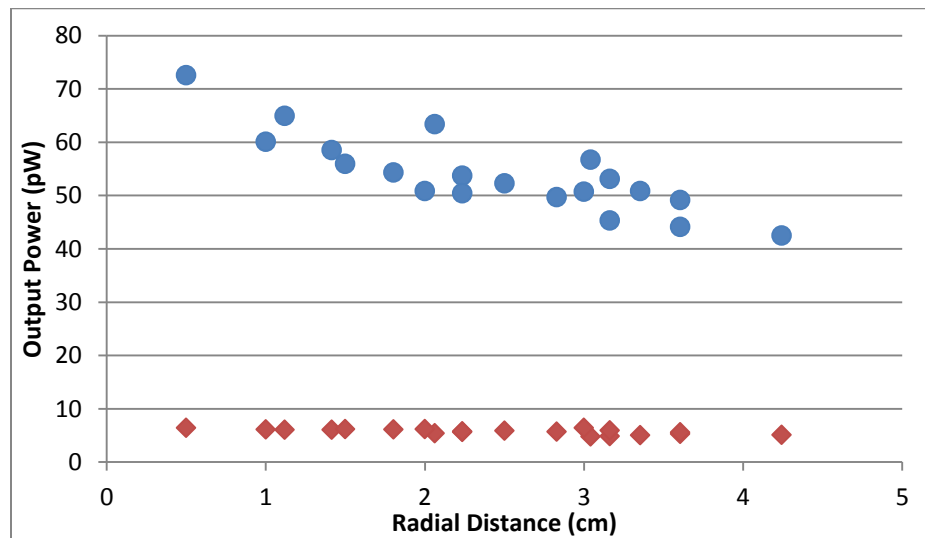


Figure 21: Proof of concept result, ● -with shield, ◆ - without shield [3]

As discussed in the methodology section, the experiment consists of two tests, with shielding and without shielding. The shielding was used to ensure there was no electric field influence on the harvester as shown in Figure 17d. Figure 21 presents the results. The without shield acquired negligibly higher power outputs which means the

influence of the electric field was much more than the magnetic field. Maximum recorded output power density was 71.28 nW/cm^3 . As the radial distance (Figure 17d) increased, the output power decreased. Since the magnets and the piezoelectric are relatively thick and stiff, there was no observable deflection. The whole assembly was held together only by the magnetic attraction force between the magnets. While the power output of the harvester is very small, it is important to keep in mind that this structure is not optimized at all, and serves only as a proof of concept.

4.1.2 Modeling Results

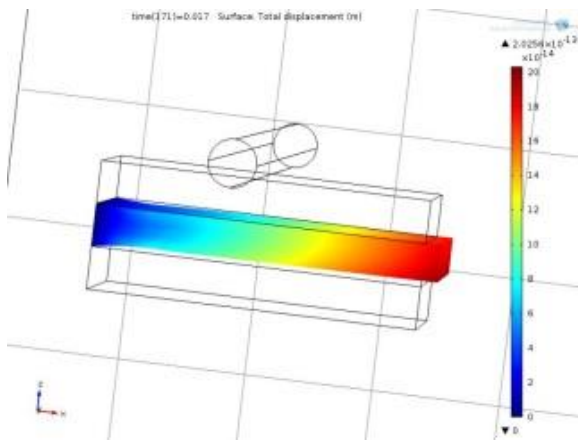


Figure 22a: Simulated displacement result [3]

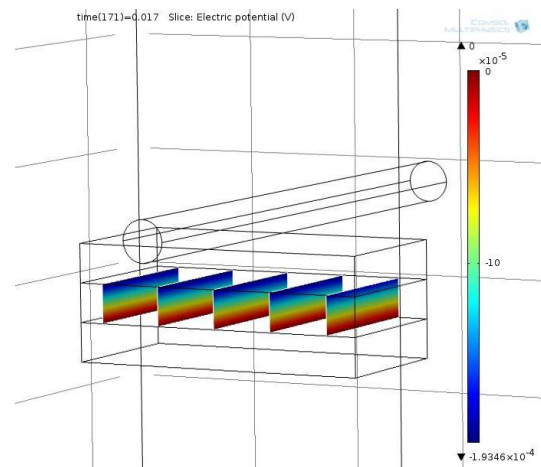


Figure 22b: Simulated output voltage result [3]

To verify the results, a model using COMSOL Multiphysics with a piezoelectric material was fit between two permanent magnets and placed in proximity of a current carrying wire. The simulated results are shown in Figures 22 and 23. Figure 22a displays a piezoelectric displacement affected by the resulting electromagnetic forces. The stress in the piezoelectric generated a voltage distribution in the vertical cross section of the

piezoelectric structure as depicted in Figure 22b. This result supports the outcome of the experiment. Figure 23a is the simulated output voltage waveform while Figure 23b is the measured output voltage waveform. The modeled output voltage peak to peak magnitude was about 13 mV, which was higher than the experimental results (1.12 mV). Both voltages have the same shape and frequency. Both also have a DC offset because of the attracting force of the two magnets that hold the harvester as one unit. The difference in magnitude comes from the air gap between the magnets and the piezoelectric materials. In addition, it was intended for the harvester to be firmly secured at the base, but slight movement was still present. From this result, a higher output voltage (or power) can be achieved by improving the mounting technique, and reducing air gap between the magnet and the piezoelectric materials.

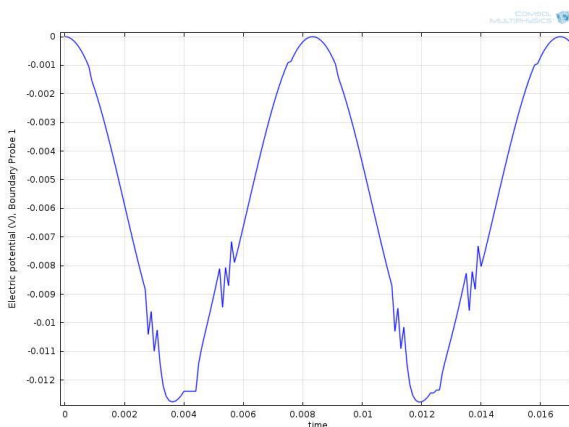


Figure 23a: Simulated output voltage waveform [3]

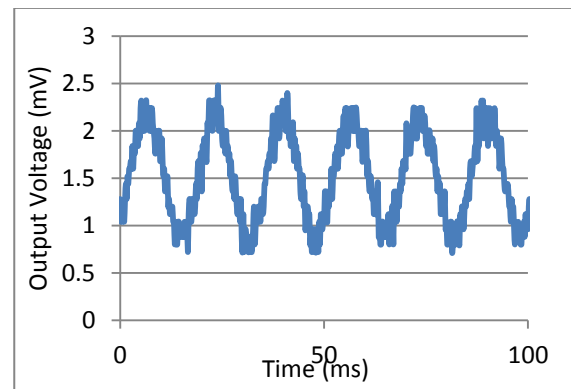


Figure 23b: Measured output voltage waveform [3]

4.1.3 Modular Design Test

Modular design gives an option of adjusting the harvesters for a certain output power. Modules can be combined in parallel or series for a higher output power. This

experiment has proved that the harvester was capable of the modular design option. Table 5 shows the results for the modular design testing. The measured output power of each harvester is shown in the second column of the table. Since the harvester was sensitive to the distance, and the location of harvester for the two cases was not exactly the same location, the output power was not the same. The theoretical power (third column) was the total sum of each harvester while the parallel combination power (fourth column) was the measured power. By observation, the theoretical total powers were close enough to conclude this harvester design can be used for modular design.

Table 5: Modular design testing

	Individual Power (pW)	Theoretical Total Power (pW)	Parallel Combination Power (pW)
2 Harvesters	70.39	136	129.96
	65.6		
3 Harvesters	136.89	381.22	342.25
	127.69		
	116.64		

4.2 High Modulus of Elasticity Materials

This section describes the test results with the harvester using low E piezoelectric materials, and distributed magnets to improve the output power density. Two different harvesters were used for all physical layout. Although the two harvesters' sizes were not the same, each of these harvesters used the same number of magnet sets and the intension was to see influence of magnet arrangements. Once the most efficient physical layout was determined, the harvester (Harvester 2) with the best performance was used to analyze for

associated impedance problem and tune for 60 Hz. The prediction for power line condition was also made using the measured results.

4.2.1 Cantilever Beam with Distributed Magnets - Physical layout I Results

According to the proof of concept test, even with the modular design option, the output power density of the harvester was still small. For this reason, physical layout I used flexible piezoelectric beam with multiple magnets added. The intension of using multiple magnets was to have as much of magnetic field interaction as possible. The physical layout I construction for Harvester 1 is shown in Figure 24 and for Harvester 2 is shown in Figure 25. The effective length (from clamping point to free end) was 12.2 cm for Harvester 1 and 7 cm for Harvester 2.



Figure 24: Harvester 1 construction for physical layout I



Figure 25: Harvester 2 construction for physical layout I

4.2.1.1 Mechanical Vibration Test

This section describes the output power responses when input vibration magnitude and frequency were changed. For the mechanical vibration magnitude experiment, the input displacement was increased and output voltages were measured.

Figure 26 presents the results for Harvester 1. For both harvesters, as the vibration magnitude raised, the output power increased. This was as expected because the harvester should produce more output power under the stronger energy source. To determine the frequency response under mechanical vibration, a displacement sinusoidal signal was used. The magnitude of the displacement was held constant while the frequency was varied. Figure 27 shows the frequency response of Harvester 1 and 2 under mechanical vibration. The resonances of Harvester 1 were at 11 and 102 Hz with corresponding output power of $231 \mu\text{W}/\text{cm}^3$ and $31.2 \mu\text{W}/\text{cm}^3$. Harvester 2's resonances were at 10 and 96.5 Hz with $0.56 \mu\text{W}/\text{cm}^3$ and $21.7 \mu\text{W}/\text{cm}^3$ respectively.

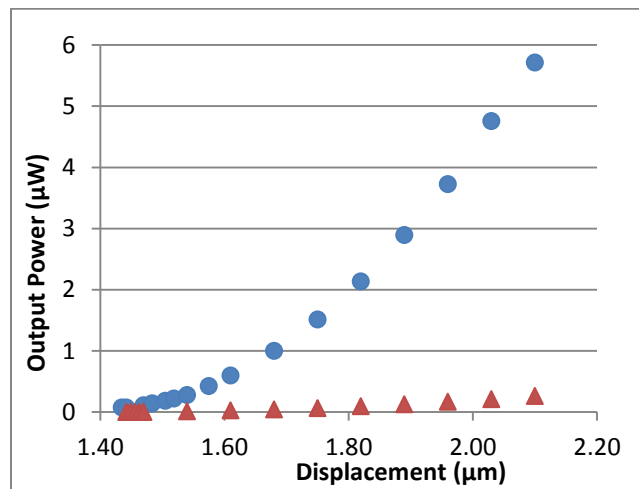


Figure 26: Varying input displacement mechanical vibration test, ● - Harvester 1, ▲ - Harvester 2

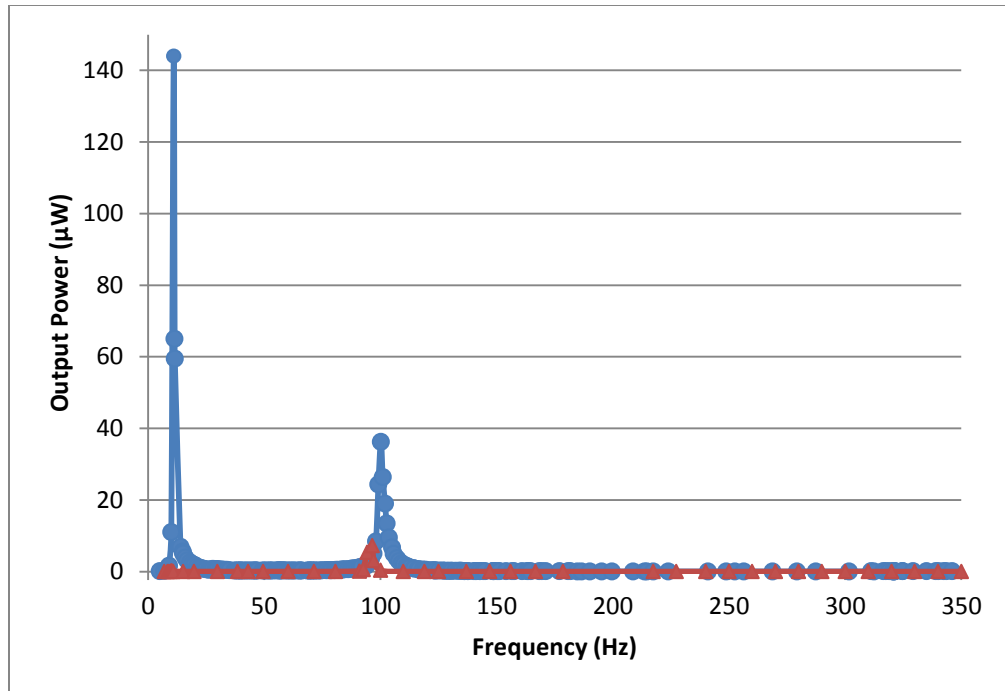


Figure 27: Varying input frequency mechanical vibration test, ● - Harvester 1, ▲ - Harvester 2

4.2.1.2 Electromagnetic Field Test

This section describes the output power responses when input current magnitude and frequency changed under EMF. In a current magnitude experiment, the frequency was kept at 60 Hz and current magnitude was varied. Figure 28 presents the output powers of both Harvester 1 and 2 as a function of input current magnitude. As seen in the input vibration magnitude experiment, as the input current magnitude increased, both harvesters output power increased. In frequency response, a current sinusoidal waveform was used; the magnitude was kept constant and frequency was varied. Figure 29 depicts the frequency response of Harvester 1 and 2 under EMF. The natural frequencies Harvester 1 were at 10.5 Hz (with $24 \mu\text{W}/\text{cm}^3$ power density) and 91 Hz (with $11.53 \mu\text{W}/\text{cm}^3$ power density). The natural frequencies Harvester 2 were at 10 Hz (with $5.83 \mu\text{W}/\text{cm}^3$ power density) and 96.5 Hz (with $214.02 \mu\text{W}/\text{cm}^3$ power density).

The natural frequencies under EMF are close when compare to the mechanical vibration. The difference could be from the mounting technique of the harvester. In the mechanical vibration test, both the holder and the harvester were mounted to the shaker and both were under vibration while in the EMF case, only the harvester was under vibration.

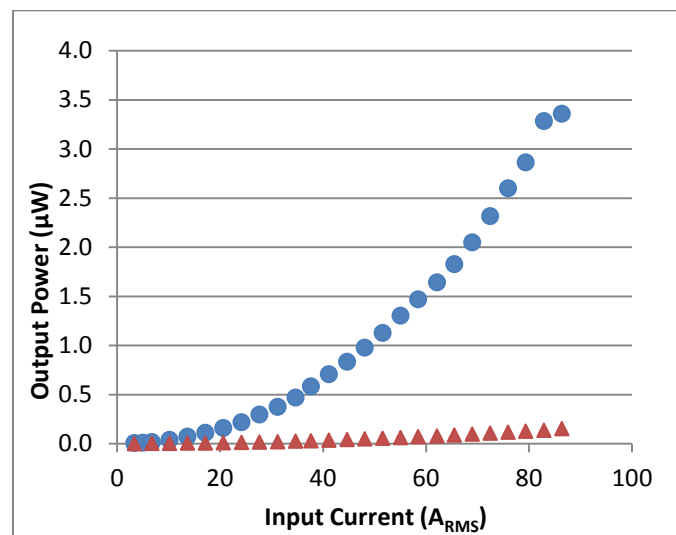


Figure 28: Varying input current EMF Test, ● - Harvester 1, ▲ - Harvester 2

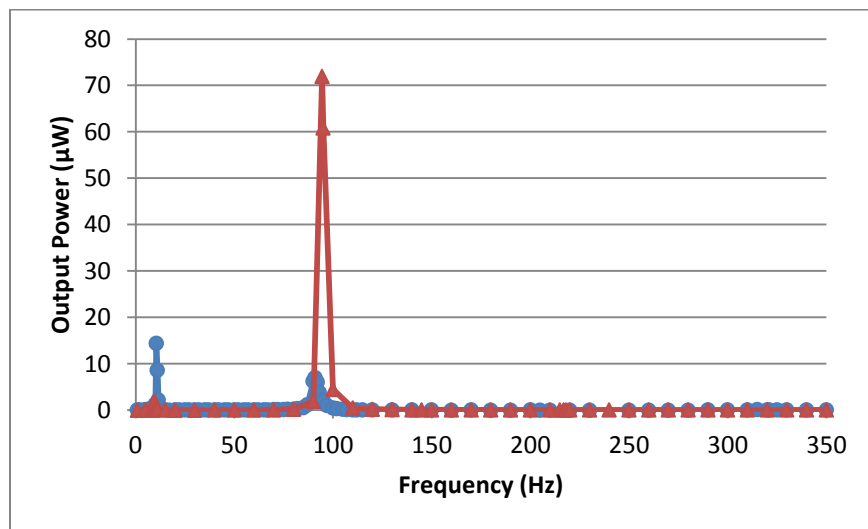


Figure 29: Varying input frequency EMF Test, ● - Harvester 1, ▲ - Harvester 2

4.2.1.3 COMSOL Multiphysics Simulation

A COMSOL Multiphysics model with the same harvester parameters of physical layout I was built for Harvester 1 and 2 to examine the frequency response of each Harvester under EMF. Figure 30 shows the simulation result for Harvester 1. Harvester 1 natural resonances were 13 and 69 Hz. These values are close to the experimental values shown in Figure 27 and 29. Unlike Harvester 1, Harvester 2 is composed of multiple layers of materials as shown in Figure 31. The modulus of elasticity of the whole harvester was not given for Harvester 2. For this reason, a modulus of elasticity (20 GPa) was selected so that this simulation result matched closely with the experiment result. The resulting natural frequencies were 13 and 95 Hz (shown in Figure 32).

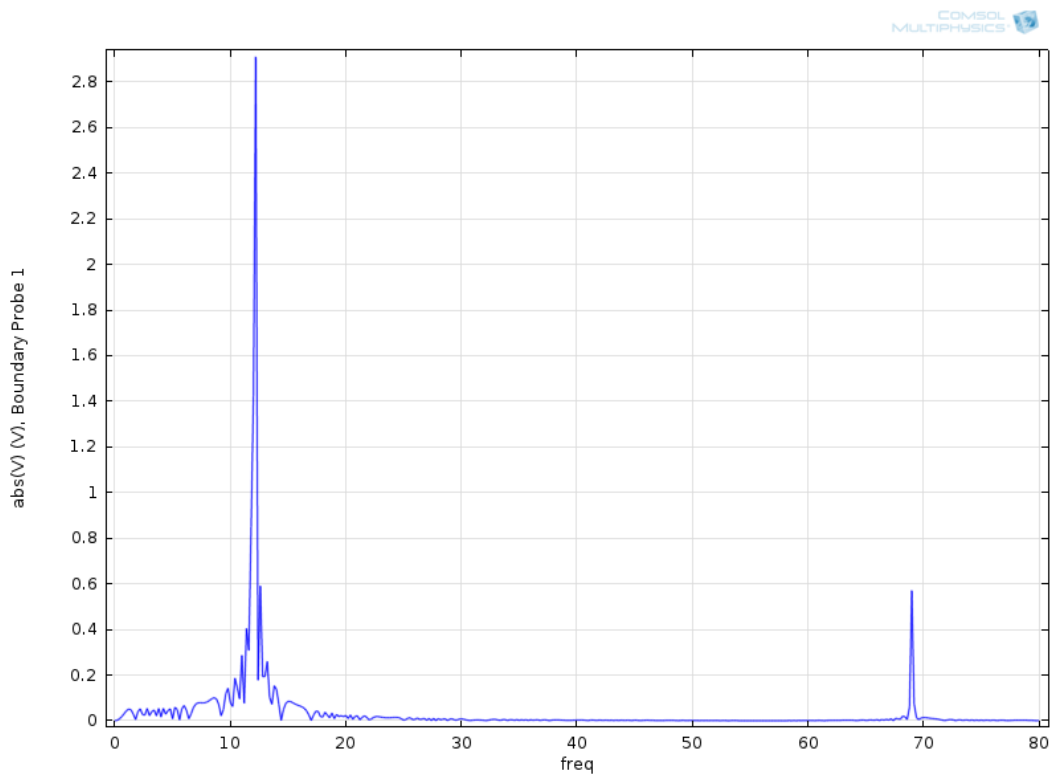


Figure 30: Frequency response of Harvester 1 simulation model under EMF - physical layout I

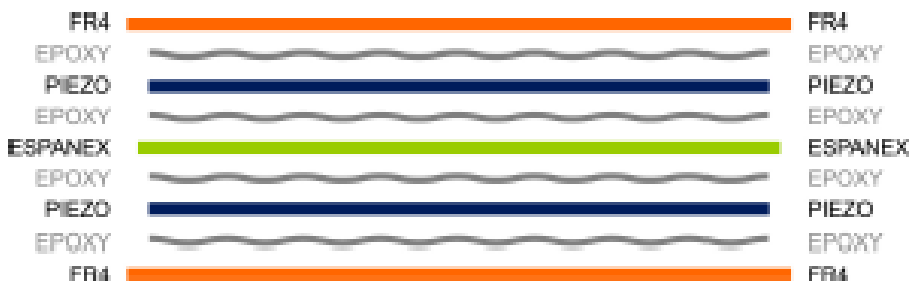


Figure 31: Harvester 2 composite [43]

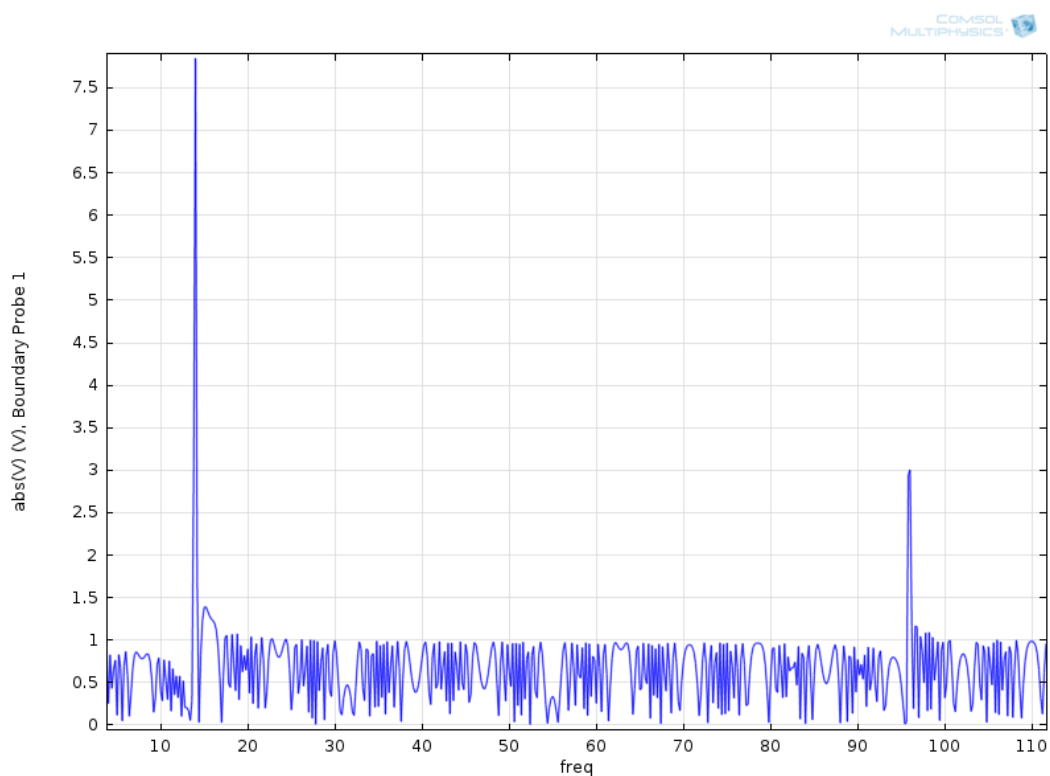


Figure 32: Frequency response of Harvester 2 simulation model under EMF - physical layout I

4.2.1.4 Effect of Distance (EMF Test Only)

The purpose of this section is to determine the optimal location to place the harvester in regard to the wire. Figure 33 presents the results when varying the vertical

distance. For both Harvester 1 and 2, as the vertical distance increased, the output power decreased. This makes sense because as the harvester is placed further away from the energy source, it should harvest less power.

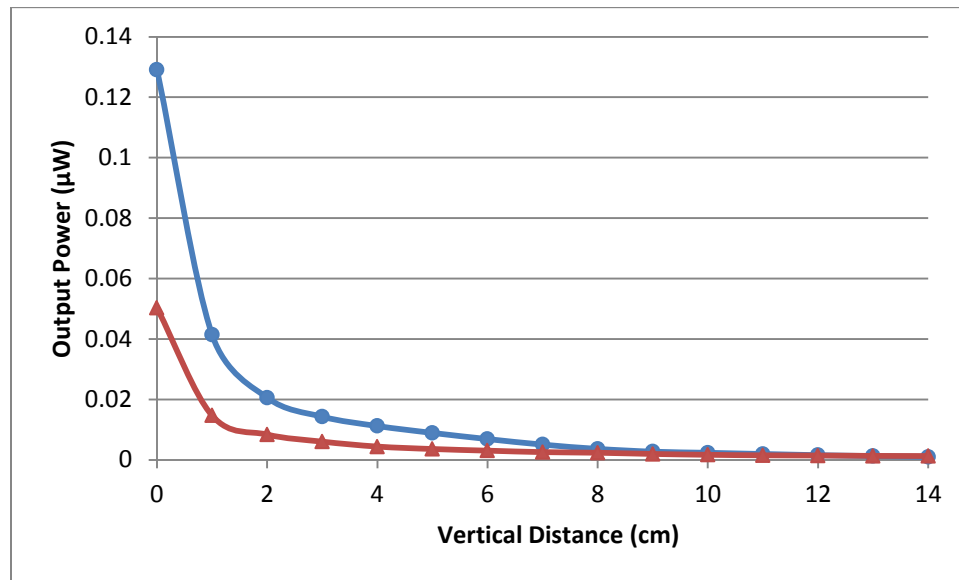


Figure 33: Varying vertical distance EMF test, ● - Harvester 1, ◆ - Harvester 2

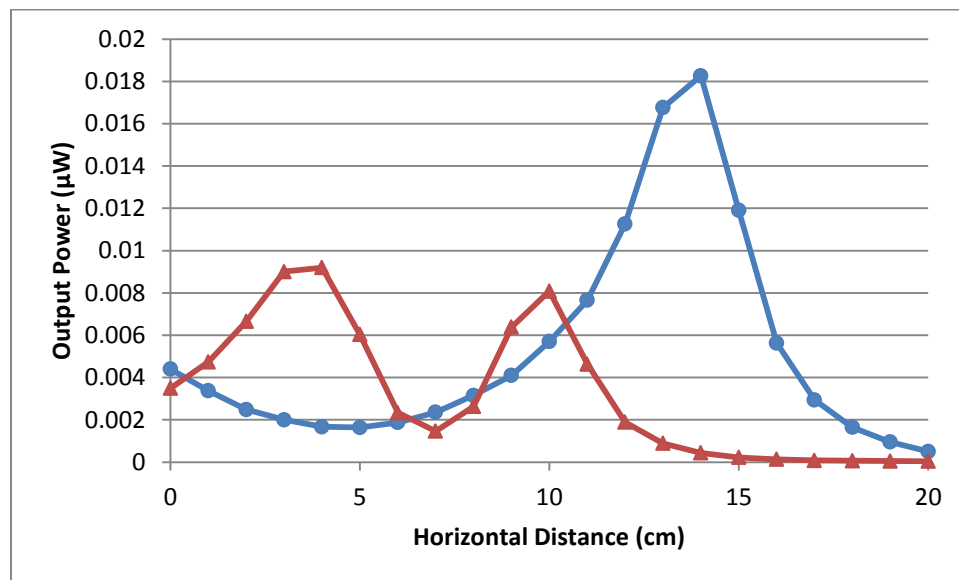


Figure 34: Varying horizontal distance EMF test, ● - Harvester 1, ◆ - Harvester 2

Figure 34 shows the device behavior when the horizontal distance (shown in Figure 19b) increased. Interestingly, the output power was at peak when the wire was under the magnets for both harvesters. There was no peak under the middle set of magnets. For Harvester 1, the middle set of magnets was too weak and poled horizontally. This middle set was used as an added mass. In Harvester 2, the distance between the middle set of magnets and the free end magnets was too close, which explains why there was no peak for when the wire was under these middle magnets.

4.2.1.5 D33 versus D31 Coupling

In this section a comparison of energy harvested using D33 and D31 modes is discussed. Figure 35 below shows the results of the test. Higher output power was obtained as the current increased due to an intensified magnetic fields interaction. The maximum output power of D33 mode was 2.23 nW and 20.68 nW for D31 mode which was about ten times less. However, this output power recorded in this test was still larger than the output power of the solid, inflexible material under the same test conditions (0.34 nW). Since the output power produced under D33 mode was not significant in comparison with D31, the rest of the tests on the harvesters were focused on D31 mode only.

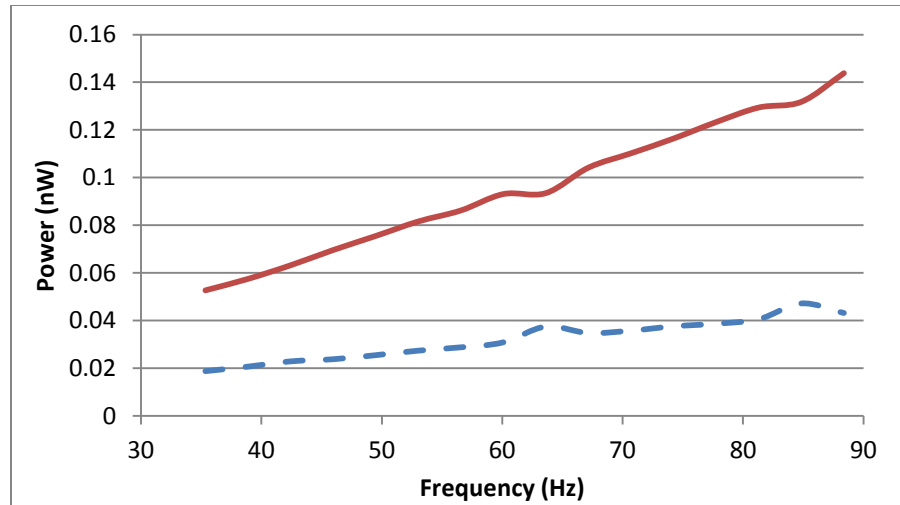


Figure 35: Harvester 1 D31 and D33 test, — — - D33 Result, — — — — — D31 Result

4.2.2 Cantilever Beam with Magnets at Free End - Physical Layout II Results

In physical layout I, although multiple magnets would help to increase the magnetic fields interaction between the wire and magnets, multiple magnets also increased the stiffness of the harvester beam. Therefore, physical layout II (Table 2) was examined. This physical configuration would allow the piezoelectric cantilever beam to deflect more and could possibly increase output power density. Both harvesters' lengths were reduced to 3 cm and used only one set of magnets as shown in Figure 36. For this layout, only the frequency response was examined since the output power responded under various vibration and current magnitudes and distances would be similar to physical layout I.

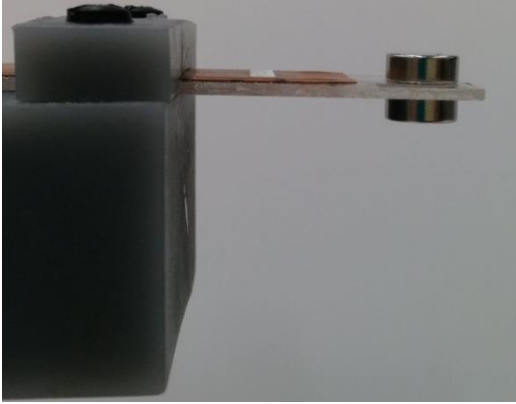


Figure 36a: Harvester 1 physical layout II

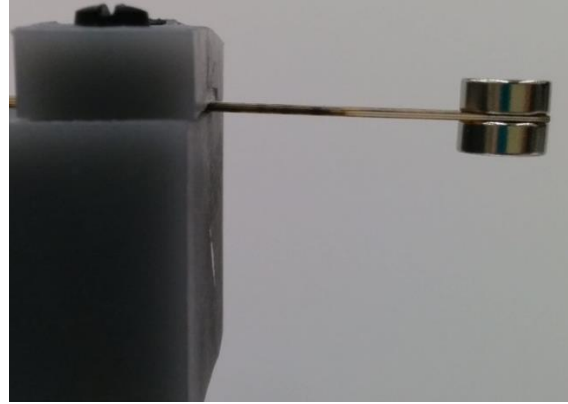


Figure 36b: Harvester 2 physical layout II

4.2.2.1 Mechanical Vibration and EMF Frequency Varying

Figure 37 shows the frequency responses of Harvester 1 (Figure 37a) and Harvester 2 (Figure 37b) under mechanical vibration. Figure 38a and 38b presents the frequency response of Harvester 1 and 2 respectively under EMF. Under mechanical vibration, the natural frequency was at 195.5 and 200.5 Hz with corresponding power density of $25.47 \mu\text{W}/\text{cm}^3$ under EMF. The frequency response of Harvester 2 is displaced in Figure 38. The natural frequency was at 81 Hz with $137 \mu\text{W}/\text{cm}^3$ power density under mechanical vibration, and 70.5 Hz with $2.14 \text{ mW}/\text{cm}^3$ under EMF. Figure 39 and 40 display the result of COMSOL modeling of Harvester 1 and 2. Harvester 1 has a natural frequency at about 197 Hz which is close to the experimental value. However, the E value of Harvester 2 was unable to adjust to match the measured natural frequency for this physical layout II.

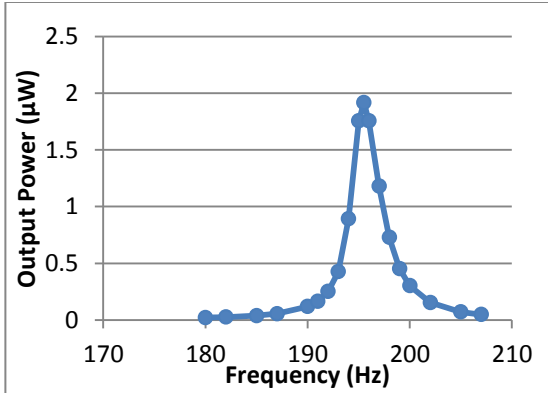


Figure 37a: Varying input frequency mechanical vibration test, Harvester 1

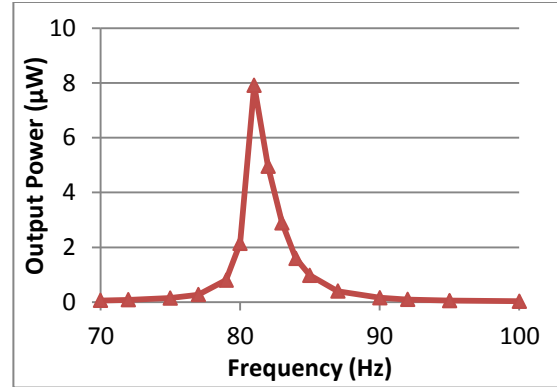


Figure 37b: Varying input frequency mechanical vibration test, Harvester 2

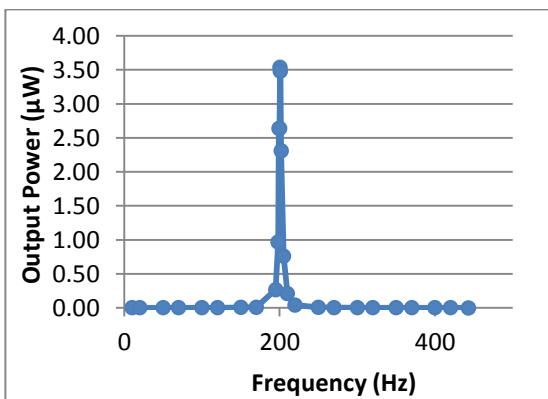


Figure 38a: Varying input frequency EMF test, Harvester 1

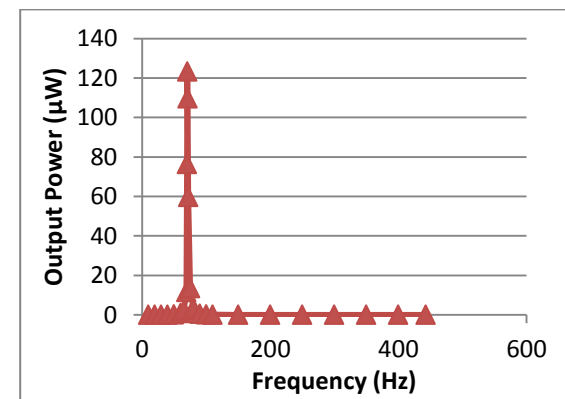


Figure 38b: Varying input frequency EMF test, Harvester 2

The natural frequency difference between the mechanical vibration and EMF could result from the mounting method of the harvester. Harvester 1 had a larger width and thickness which result in a higher moment of inertia; hence, Harvester 1 had higher natural frequency (based on Equation 1 and 2). Under mechanical vibration, Harvester 1 produced a lower output power density in the physical layout II than the physical layout I; however, under EMF, higher output power was obtained in physical layout II. Harvester 2 produced a higher power density in both mechanical vibration and EMF. Furthermore, the output power density of Harvester 2 increased significantly under EMF (about 10 times more). One reason that could contribute to a high power density could be

the small thickness and an increase in flexibility by reducing the number of magnets used for Harvester 2. The same conclusion could not be drawn for Harvester 1 since this harvester's size and added magnets were changed completely. However, the changing in magnets mass from 27.43 g (total of all magnets' mass) to 3.2 g (total of 2 cylindrical magnets' mass) is believed to be the cause of a lower power density.

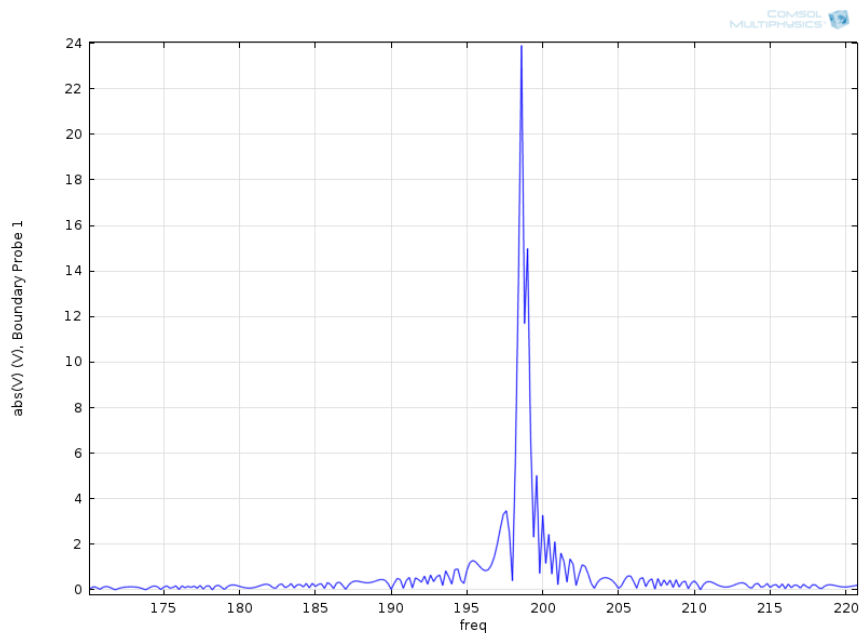


Figure 39: Frequency response of Harvester 1 simulation model under EMF - physical layout II

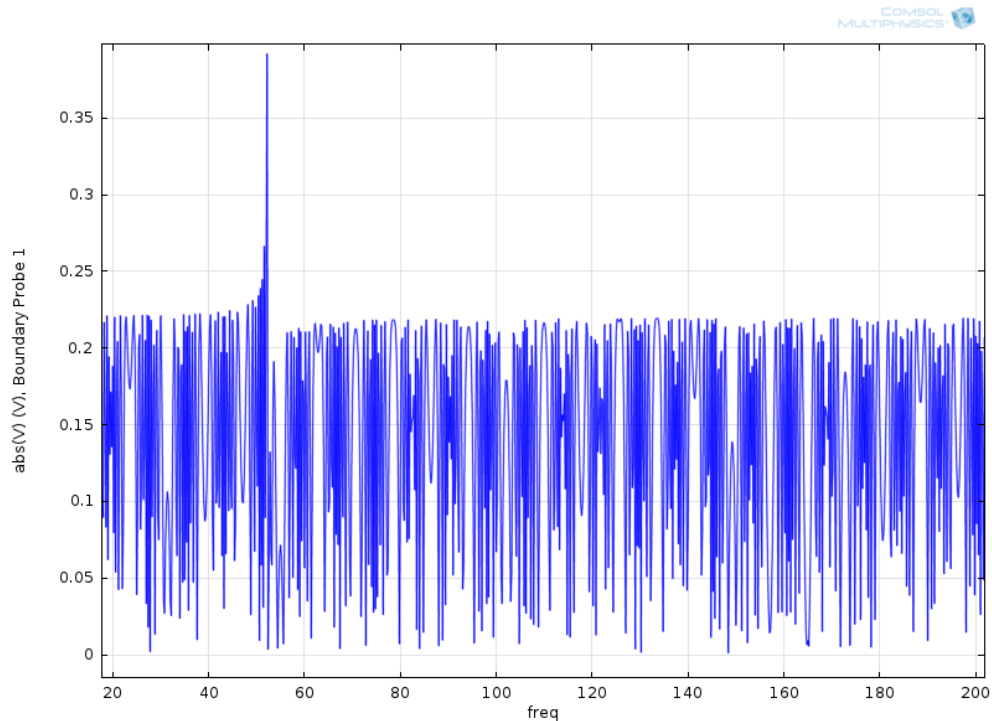


Figure 40: Frequency response of Harvester 2 simulation model under EMF - physical layout II

4.2.3 Increasing Magnetic Fields Interactions – Physical Layout III

Although physical layout II showed an improvement on output power, magnetic interactions of this physical layout was not as good as physical layout I. With the observation seen in physical layout II, the same magnet and harvesters' size with physical layout II were kept the same so that there was stiffness added to the harvester beam. A 1 x 1/2 x 1/8 inch magnet, (magnet A in Table 4) was added at the bottom magnet C (Table 4) to increase the mass and magnetic fields interaction strength without affecting the flexibility of the beam. The magnet C has a residual induction of 12200 Gauss while the added magnet A has a residual induction of 13200 Gauss. However, the surface field of magnet A is higher than the cylindrical magnet due to a larger surface area. According to Equation 4 and Figure 15, the longer the interaction length between the magnet and wire,

the higher the EMF interactions were. To ensure that the mass did not have an influence on the increase of output power, the bottom magnet was placed perpendicular (Figure 41a and 43a) and parallel (Figure 42a and 44a) to the wire. For this test, both harvesters were examined when input frequency was varied while the input current and position stayed constant.

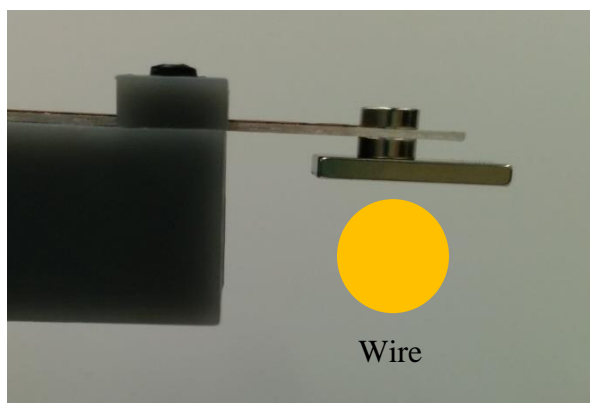


Figure 41a: Harvester 1 with bottom magnet placed perpendicular to the wire

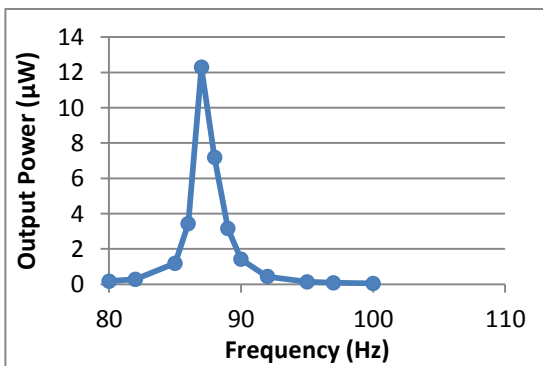


Figure 41b: Frequency varying mechanical vibration test

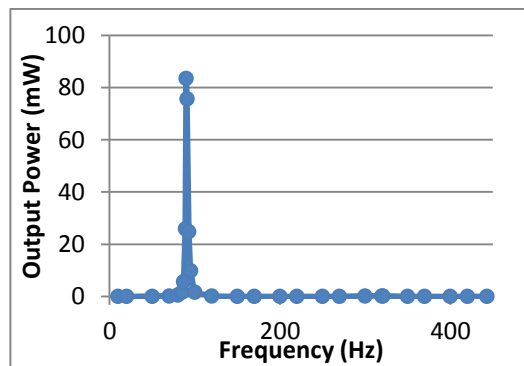


Figure 41c: Frequency varying EMF test

Figure 41 shows the frequency response of Harvester 1 with the bottom magnet placed perpendicular to the wire. The natural frequency was at 87 Hz with $162.6 \mu\text{W}/\text{cm}^3$ output power density under mechanical vibration and at 90 Hz with $1.1 \text{ mW}/\text{cm}^3$ under

EMF. The natural frequency measured under mechanical vibration and EMF are close. The results of Harvester 1 with the bottom magnet placed parallel to the wire are shown in Figure 42. Under mechanical vibration, the natural frequency was 92 Hz with $150.3 \mu\text{W}/\text{cm}^3$ and 93 Hz with $1.61 \text{ mW}/\text{cm}^3$ under EMF.

Different configurations of mounting the harvester in mechanical vibration tests and EMF tests could cause a difference in measured natural frequency under the both sources of energy. The natural frequency in the case of parallel placing the bottom magnet was slightly higher for the perpendicular placing. The output power for both cases under mechanical vibration was similar (162.6 and $150.3 \mu\text{W}/\text{cm}^3$). The difference in these output power values could come from errors in oscilloscope readings. However, under the EMF source, the output power of the parallel placing was higher than the perpendicular placing (1.61 and $1.1 \text{ mW}/\text{cm}^3$ respectively). This proved that the magnetic fields interaction increased by increasing the interaction length between the wire and magnets which confirmed Equation 4 and Figure 15.

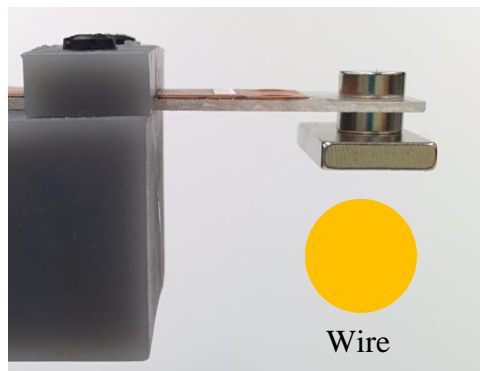


Figure 42a: Harvester 1 with bottom magnet placed parallel to the wire

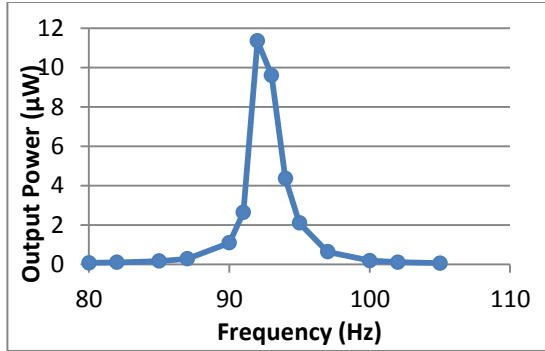


Figure 42b: Frequency varying mechanical vibration Test

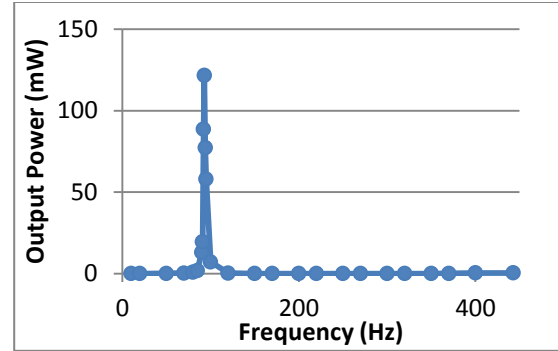


Figure 42c: Frequency varying EMF test

The same set of tests was conducted for Harvester 2. The identical magnet configurations were used. Results of the perpendicular placing of the bottom magnet are shown in Figure 43b and 43c. For mechanical vibration, the natural frequency was 36 Hz and 142 Hz with 0.91 mW/cm^3 and 19.64 µW/cm^3 power density (respectively). For EMF, the resonance was 33 Hz and 156 Hz with 13.74 mW/cm^3 and 0.58 mW/cm^3 . Figure 44b and 44c presents the results of the parallel placing of the bottom magnet. The resonance was at 34 Hz and 187 Hz with a corresponding power output of 0.78 mW/cm^3 and 39 µW/cm^3 under mechanical vibration. Under EMF, the natural frequency was at 20 Hz and 208 Hz with 15.7 mW/cm^3 and 0.47 mW/cm^3 output power.

Harvester 1 and 2 displayed similar behavior. Output power for the perpendicular placed bottom magnet was higher than the parallel placed magnet under mechanical vibration. However, the output power density increased in the case in which the bottom magnet was positioned parallel to the wire under EMF. Once again, this proved the magnetic fields interaction was increased under the parallel placing of the bottom magnet since the mass and magnets used were the same. Maximum recorded output power density was 15.7 mW/cm^3 (Harvester 2 in EMF) which was approximately seven times

higher than the maximum output power density for physical layout II (of the same Harvester 2 in EMF). By observation, Harvester 2 produced a much higher (about 10 times) output power density than Harvester 1. Therefore, Harvester 2 with this configuration was used to examine loading electrical investigation and to tune to 60 Hz.

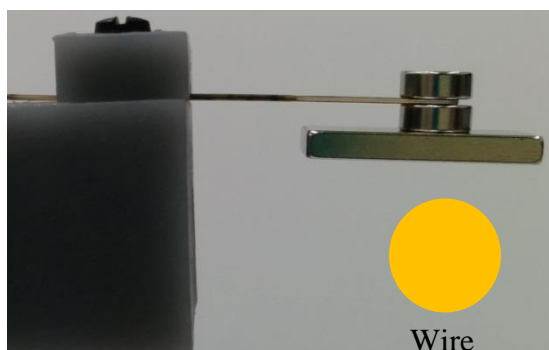


Figure 43a: Harvester 2 with bottom magnet placed perpendicular with the wire

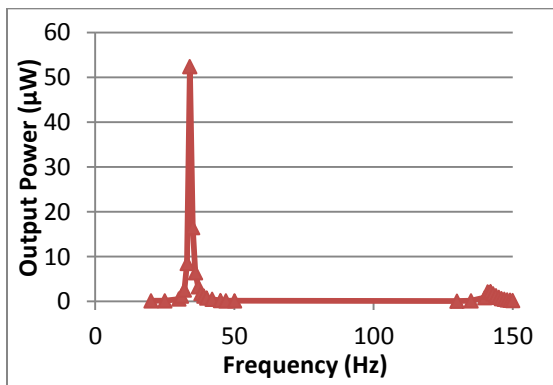


Figure 43b: Frequency varying mechanical vibration test

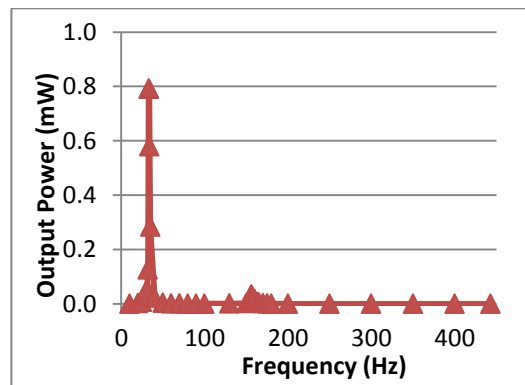


Figure 43c: Frequency varying EMF test

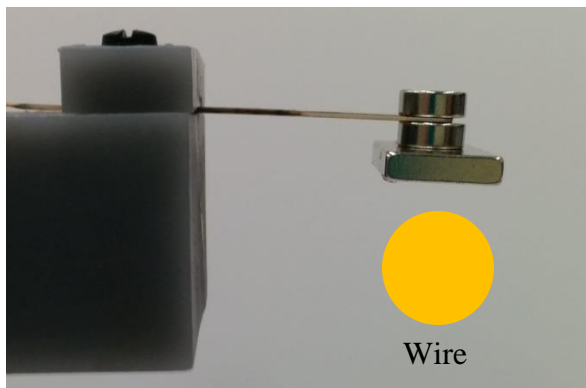


Figure 44a: Harvester 2 with bottom magnet place parallel with the wire

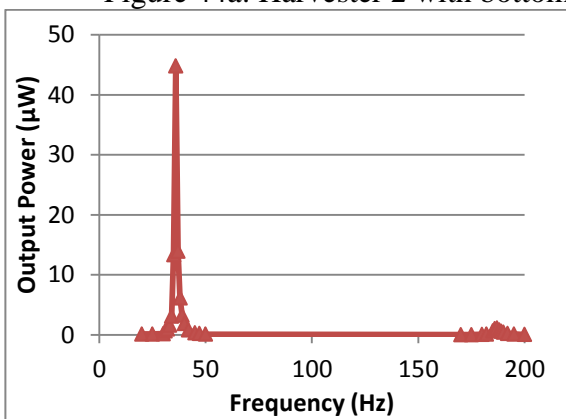


Figure 44b: Frequency varying mechanical vibration test

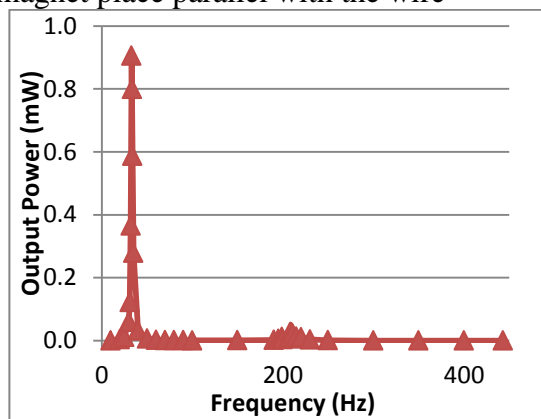


Figure 44c: Frequency varying EMF test

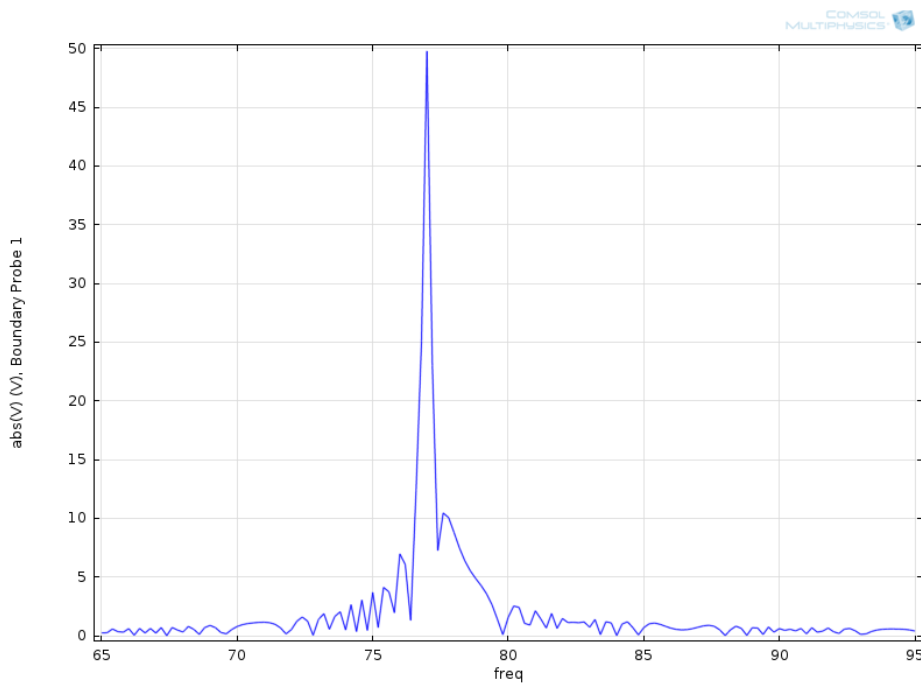


Figure 45: Frequency response of Harvester 1 simulation model under EMF - physical layout III with bottom magnet placed perpendicular with the wire

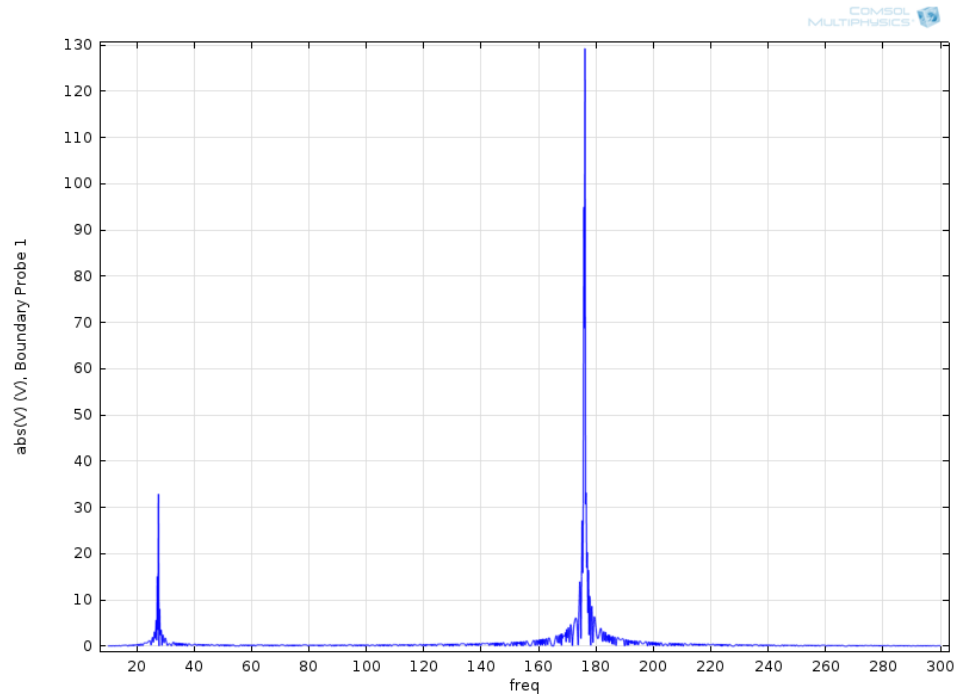


Figure 46: Frequency response of Harvester 2 simulation model under EMF - physical layout III with bottom magnet placed perpendicular with the wire

Figure 45 and 46 present the simulated frequency response of Harvester 1 and 2 (respectively) for physical layout III (Table 2) with bottom magnet placed perpendicular with the wire. The natural frequency of Harvester 1 was about 77 Hz. This is smaller than the measured value but it is still close. The natural frequency of Harvester 2 was 29 Hz and 178 Hz. The first natural frequency is close but the second value is higher. The output voltages of Harvester 2 are much higher than measured values. The reason for this could be the modulus of elasticity used for physical layout was not close for this case.

Figure 47 and 48 show the simulated Harvester 1's and 2's frequency response for physical layout III with the bottom magnet placed parallel with the wire respectively. The simulated resonance of Harvester 1 was about 86.5 Hz while the simulated resonances of Harvester 2 were about 35 Hz and 289 Hz. Similarly, resonance of Harvester 1 was close

to the experiment value. The second resonance of Harvester 2 is higher than experimental value and the output voltages are high. The E value was not determined to match the natural frequencies of Harvester 2 for this layout configuration.

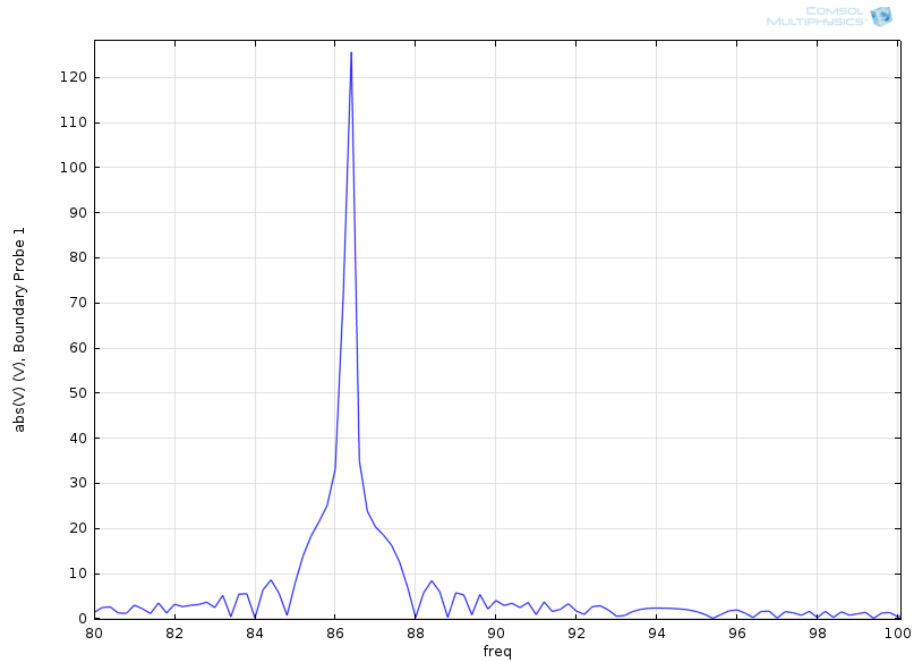


Figure 47: Frequency response of Harvester 1 simulation model under EMF - physical layout III with bottom magnet placed parallel with the wire

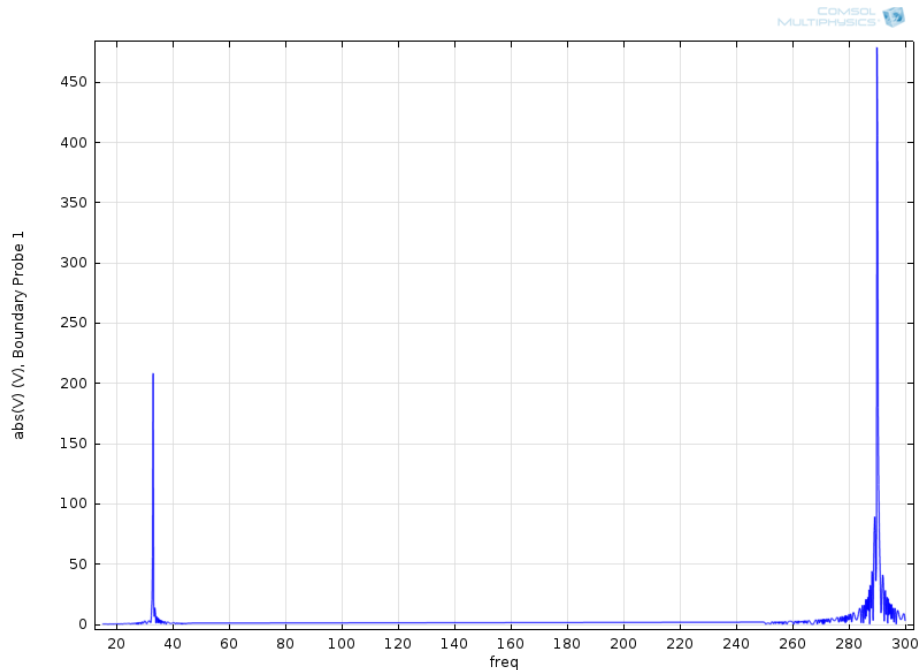


Figure 48: Frequency response of Harvester 2 simulation model under EMF - physical layout III with bottom magnet placed parallel with the wire

4.2.4 Harvester 2 Impedance Problem

Figure 49b shows the results of the impedance test. Due to oscilloscope reading capability, the series case of 1X probe reading was out of range for loading that is bigger than $1\text{ M}\Omega$. The output voltage across a resistor load that smaller than $1\text{ M}\Omega$ matched closely. Above $1\text{ M}\Omega$, the loading impedance was larger enough to be considered as open voltage. For this same reason, the output power of the series case was almost twice of the parallel case. Since all the loading used in the previous testing was $1\text{ M}\Omega$ and below, there was no correction factor needed. The same result was also used to study for the maximum power transfer as shown in Figure 49c. In series connection the maximum power was achieved with a load of $200\text{ k}\Omega$ and $500\text{ k}\Omega$ for parallel connection.

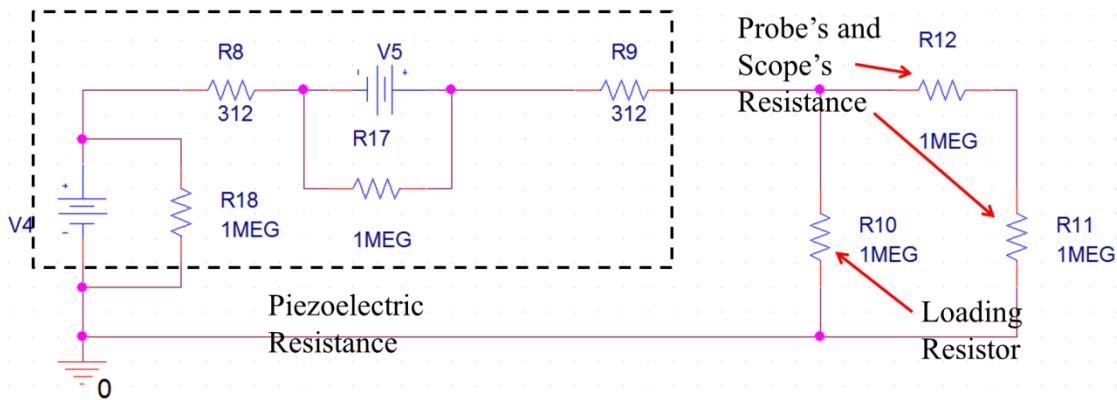


Figure 49a: Harvester and measuring equipment resistance model

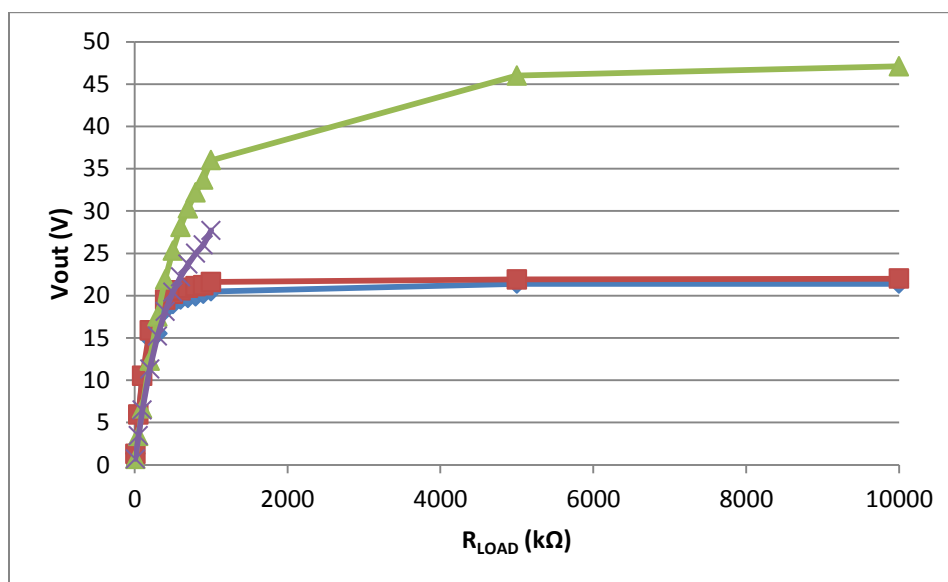


Figure 49b: Loading test, \blacktriangle - series connection with 10X probe reading, \times - series with 1X probe reading, \blacksquare - parallel connection with 10X reading, and \blacklozenge - parallel connection with 1X reading

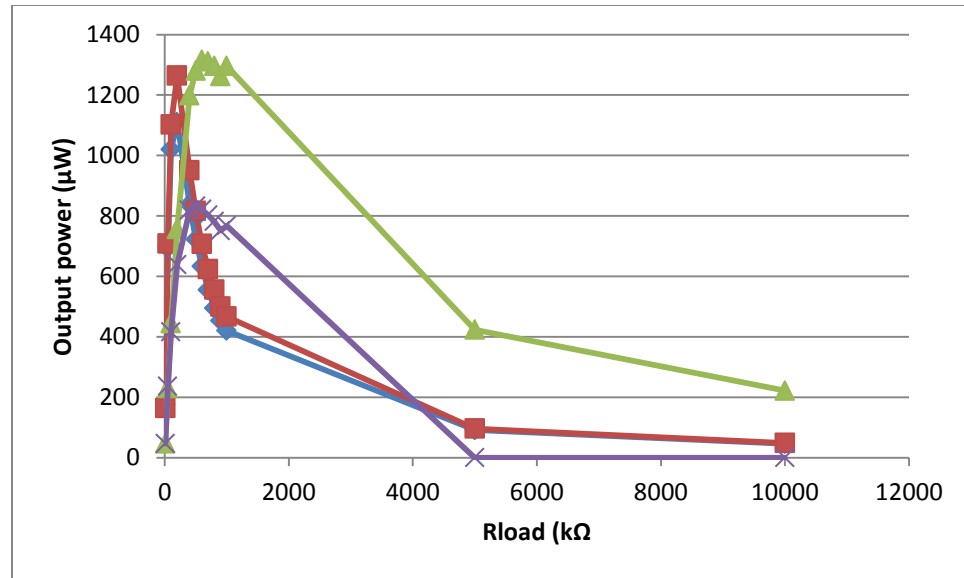


Figure 49c: Maximum power transfer results, ▲ - series connection with 10X probe reading, × - series with 1X probe reading, ■ - parallel connection with 10X reading, and ◆ - parallel connection with 1X reading

4.2.5 Electrical Impedance Resonance Influence

This section presents the result of the electrical impedance resonance to ensure that the electrical impedance of the harvester and the measurement equipment did not have influence of the measured output power. As shown in Figure 50, the equivalent impedance model of the entire system for Harvester 1 and 2. Figure 51 presents the Pspice simulation frequency response of Harvester 1 and 2 including the measuring equipment impedances. The resonance frequency of Harvester 1 was at 1659.6 kHz while resonance frequency of Harvester 2 was at 1665.6 kHz. These resonances are higher than the operating frequency (60 Hz to 180 Hz). For this reason, the electrical impedance resonance does not have an effect on the output power.

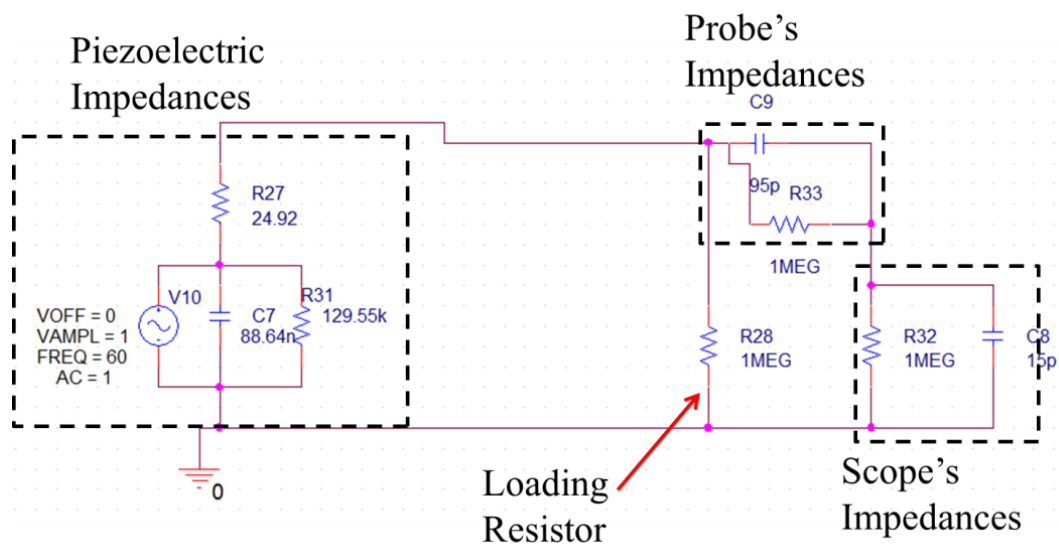


Figure 50a: Pspice impedance model of Harvester 1 and measuring equipment

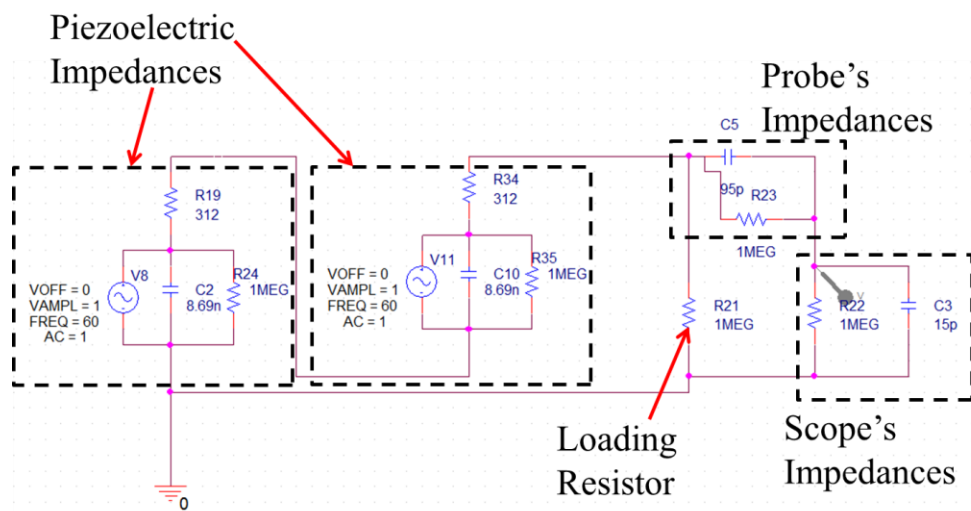


Figure 50b: Pspice impedance model of Harvester 2 and measuring equipment

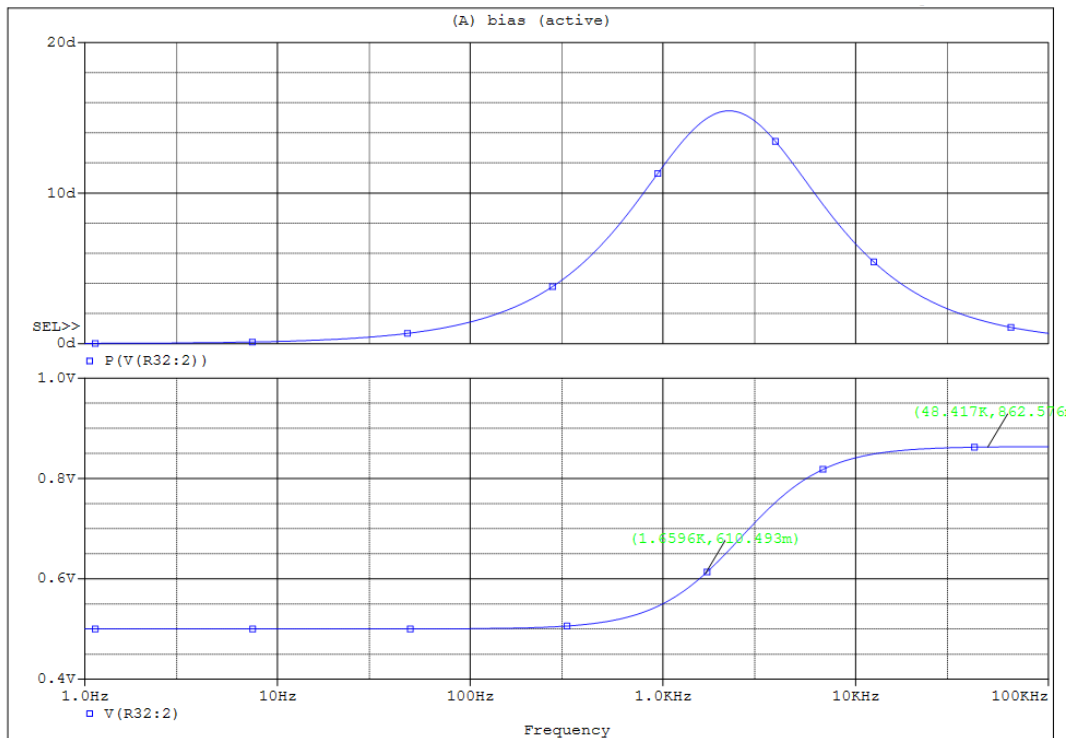


Figure 51a: Simulated frequency response of Harvester 1

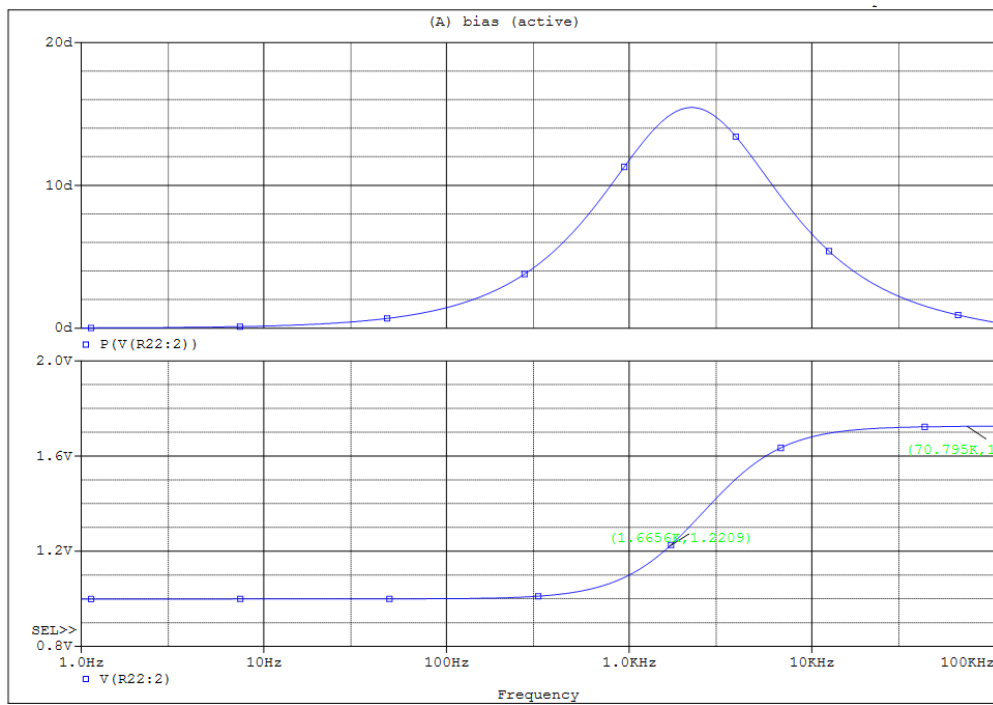


Figure 51a: Simulated frequency response of Harvester 2

4.1.1 Tuning for 60Hz

One goal for this research was to harvest the wasted electromagnetic energy of the power line. The output power of physical layout IIIB was significantly improved; however, the natural resonances of this physical layout were not at 60 Hz. For this reason, Harvester 2 was needed to tune to 60 Hz. There were two options to tune to a desired frequency without changing the harvester, changing the weight of the added mass or length of the harvester. Changing the length was chosen for this test. An effective length of 2.2 cm was used for Harvester 2. The frequency response of Harvester 2 and output power responses under various magnitudes of excitation under mechanical vibration and EMF were examined.

Figure 52 presents the frequency response of Harvester 2. The first natural resonance was 66 Hz under mechanical vibration and exactly 60 Hz under EMF. Other natural frequencies were 301 Hz and 379 Hz (under mechanical vibration) and 342 Hz (under EMF). Figure 53 shows the response of Harvester 2 under various vibration and current magnitude. As expected, as the source strength increased, the output power increased. Highest output power was 2.9 mW (31.87 mW/cm³ density) under 88 A_{RMS} current and 409 μW (4.491 mW/cm³) under 1.4 mm displacement of mechanical vibration.

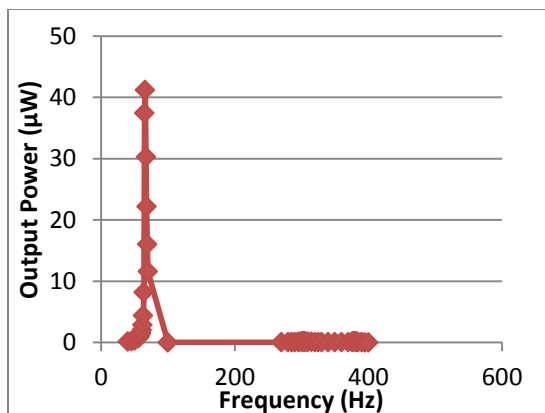


Figure 52a: 60 Hz tuning frequency response under mechanical vibration

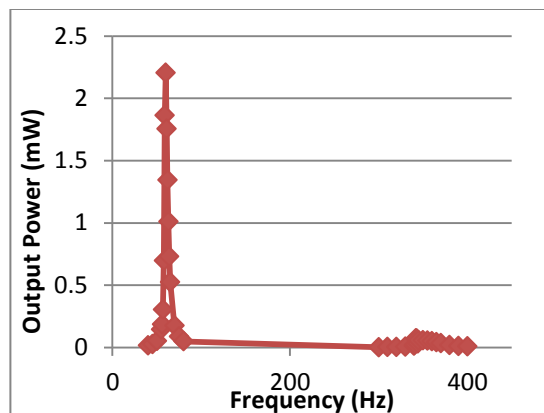


Figure 52b: 60 Hz tuning frequency response under EMF

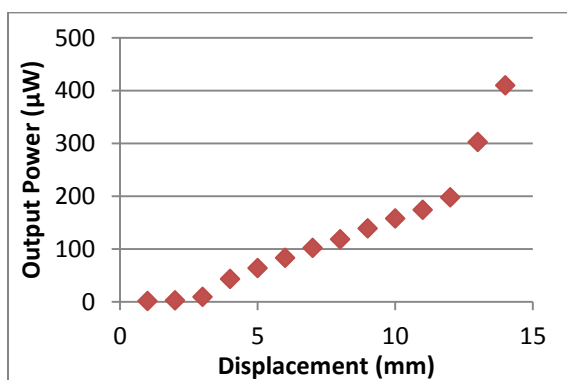


Figure 53a: 60 Hz tuning output power versus vibration magnitude

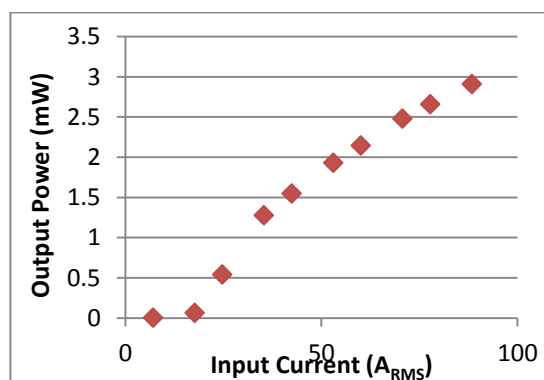


Figure 53b: 60 Hz tuning EMF output power versus current magnitude

4.2.6 Sources Combination Test

This section describes the harvester behavior under both mechanical vibration and EMF. Figure 54 shows the output voltage across Harvester 2 under both sources' influences. By inspection, the output voltage was not exactly a sinewave. This happened due to the slightly difference in frequency or phase shift. Table 6 displays the testing result when both mechanical vibration and EMF source are present. Output voltage was measured with each source present separately. Results are shown in column 2 for EMF and column 4 for mechanical vibration. A theoretical averaged output voltage was calculated based on the results in column 2 and 4 by taking the root mean square value of

the sum the two waveforms with a frequency difference of 0.3 Hz. This theoretical value is reported in column 5. The output power was shown in column 5. Column 6 and 7 were the measured combination output voltage and power under the experiment. By observation, the measured combination output voltages were close to the theoretical value in all three various source strength. The output power showed a higher difference between theoretical and measure since this power has a quadratic relationship with the voltage.

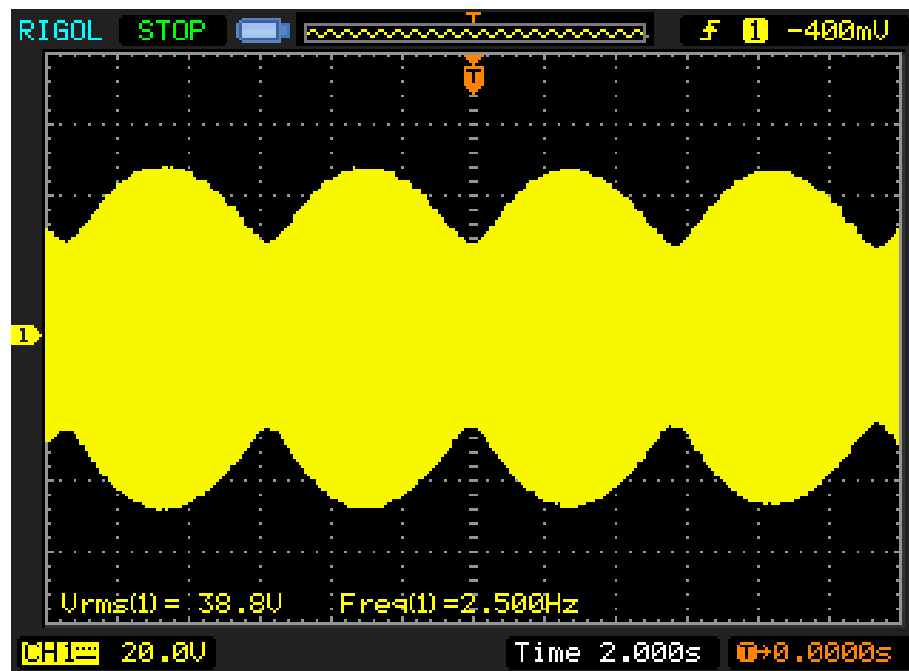


Figure 54: 60 Hz tuning mechanical vibration source strength test

Table 6: Combination sources testing results

EMF		Mechanical Vibration		Combination Theoretical		Combination Measured	
Input Current (A_{RMS})	Output Voltage (V_{RMS})	Input Displacement (mm)	Output Voltage (V_{RMS})	Output Voltage (V_{RMS})	Output Power (mW)	Output Voltage (V_{RMS})	Output Power (mW)
35.35	20.50	0.73	15.10	33.40	2.79	33.30	2.77
53.03	26.70	0.73	15.10	39.36	3.87	38.20	3.65
70.70	29.70	0.73	15.10	42.27	4.47	38.80	3.76

The output power increased with both sources, and the maximum output power was 3.76 mW (35.64 mW/cm³). With this output power value, it would take about 35 harvesters connected together to produce the amount of power needed for the sensor under the condition tested in the laboratory. However, the condition in the power line environment has a higher displacement of vibration and higher current.

4.2.7 Prediction for Power Line Environment

As stated previously, the harvester will be used to harvest energy to supply the sensor on power line. Unfortunately, the combination testing condition used could not match the power line environment due to limitation in equipment. For this reason, the output voltage versus input mechanical vibration and current magnitude data was used to predict the output power when working under the power line environment. Shown in Figure 55 are the output voltages with a MATLAB fitted curve under mechanical vibration, and Figure 56 are the output voltages with a fitted curve under EMF.

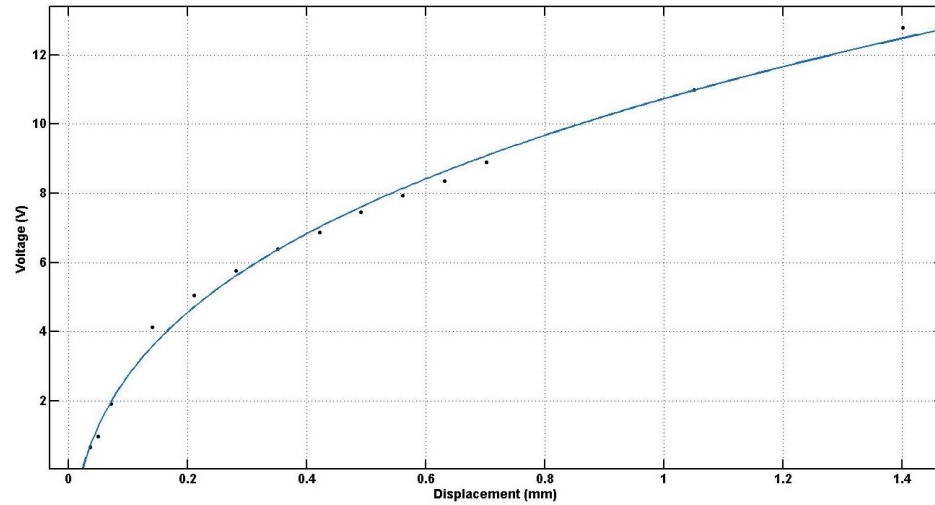


Figure 55a: 60 Hz tuning mechanical vibration source strength test

General model Power2:
 $f(x) = a*x^b+c$
 Coefficients (with 95% confidence bounds):
 a = 15.35 (12.61, 18.09)
 b = 0.3204 (0.2306, 0.4102)
 c = -4.615 (-7.434, -1.796)

Goodness of fit:
 SSE: 0.8398
 R-square: 0.9949
 Adjusted R-square: 0.994
 RMSE: 0.2763

Figure 55b: Parameter of fitting curve under various mechanical vibration magnitudes

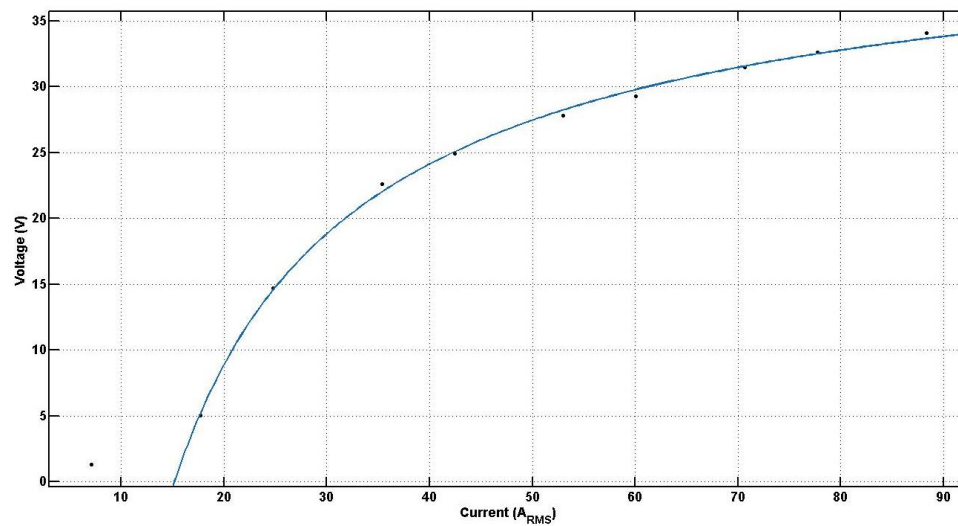


Figure 56a: 60 Hz tuning EMF source strength test

General model Power2:
 $f(x) = a*x^b+c$
Coefficients (with 95% confidence bounds):
a = -404.5 (-533.8, -275.3)
b = -0.8146 (-1.012, -0.6175)
c = 44.16 (36.29, 52.03)

Goodness of fit:
SSE: 22.5
R-square: 0.9815
Adjusted R-square: 0.9762
RMSE: 1.793

Figure 56b: Parameter of fitting curve under various current magnitudes

Table 7: Prediction of harvested power for power line environment

EMF		Mechanical Vibration			Prediction	
Input Current (A)	Output Voltage (V_{RMS})	Input Displacement (mm)	Frequency (Hz)	Output Voltage (V_{RMS})	Output Voltage (V_{RMS})	Output Power (mW)
100.00	31.56	0.18	150	4.24	31.83	2.53
100.00	31.56	0.18	60	4.24	35.79	3.20
600.00	41.23	17.96	150	38.62	53.49	7.15
600.00	41.23	17.96	60	38.62	75.32	14.18

With the information about the environment of the power line and the relationship between output voltage and various sources strength, a prediction of output power was made, shown in Table 7. The output voltage in column 2 of Table 7 is the estimated output voltage based on the fitted curve of Figure 51 with the input current in column 1. Output voltage in column 5 was estimated with the fitted curve in Figure 52. The prediction voltage was the root mean square value of the sum of the voltage in each source. The current frequency was assumed to be exactly 60Hz. With the minimal condition which input current is 100 A and vibration displacement of 0.18 mm and frequency at 150 Hz, the predicted output power is 2.53 mW. However, with the same

condition but frequency was exactly at 60 Hz for both sources, the predicted output power increased to 3.2 mW. With maximum condition of 600 A current and 17.96 mm displacement, the predicted output power is 7.15 mW at 150 Hz mechanical vibration frequency and 14.18 mW at 60 Hz mechanical vibration frequency. With this prediction, to produce enough power to supply the sensor, it would need about 10 harvesters. Since there are huge amount of current and vibration, it is important to ensure that the harvester material can be able to handle the amount of stress induce on it.

CHAPTER 5: CONCLUSIONS

5.1 Discussion

The main purpose of this research is to harvest unused energies in the power line environment to power a sensor that requires approximately 130 mW to function.

Mechanical vibration and electromagnetic field are two strong sources of energy present in this environment. The proposed energy harvester was used to harvest both mechanical and electromagnetic field energy. The proof of concept results confirmed that the idea of using permanent magnets placed close to a wire to retrieve energy was possible.

However, the output power obtained was small due to material stiffness. Therefore, it had been decided to use flexible material.

Two different flexible piezoelectric cantilever beams were used to test. One was built with macro fiber composite piezoelectric and polycarbonate (Harvester 1). The other (Harvester 2) was a commercial product with two piezoelectric layers, FR4, epoxy, and espanex (shown in Figure 31). The piezoelectric materials were connected in series used for all tests except for the investigation of impedance for Harvester 2. The two harvesters were combined with magnet as an added mass and a medium to deflect the piezoelectric material in electromagnetic field were used. Three arrangements of magnets were called physical layout I, II, and III. The testing for these physical layouts consists of an electromagnetic and mechanical vibration response tests. Based off the test results, the

harvester with the most efficient physical layout was used to tune to 60 Hz and tested for a combination of both mechanical and electromagnetic field energy source.

Table 7 summarizes the resonances, and output power density for Harvester 1 and 2 with all physical layouts. All harvesters that used flexible materials were able to harvest energy from both sources of energy. Output power was highest at position which the wire was closest to the free end side of the harvester. The difference in the measured natural frequencies under mechanical vibration and electromagnetic depends on the way the harvester was mounted. In mechanical vibration, both the holder and harvester were vibrated. Only the harvester beam was vibrated in electromagnetic field. Piezoelectric working modes (D31 and D33 mode) were also examined with Harvester 1. The output power of D33 mode was smaller than D31 mode, at the same time, output power of D31 mode increased at a faster rate than D33 mode as the input current increased. Harvester 1 was able to produce output power in both mode but D33 mode was not efficient. For this reason, the main focus for the rest of the testing was to operate in D31 mode.

Since Harvester 2 includes 2 piezoelectrics embedded in the system and is smaller in size, the performance of Harvester 2 was better in EMF. Having distributed multiples magnets helped to increase the mass and magnetic interaction but decreased the deflection of the beam; physical layout II proved that. The most efficient structure was physical layout IIIB. Adding a bigger magnet at the bottom of the free end magnet (as shown in Table 4) increased the mass and magnetic interaction without affecting the deflection of the harvester beam.

Table 8: Experiment summary

	Harvester 1						Harvester 2				
	Mechanical Vibration			EMF			Mechanical Vibration			EMF	
	Resonance Frequency (Hz)	Output Power ($\mu\text{W}/\text{cm}^3$)	Resonance Frequency (Hz)	Resonance Frequency (Hz)	Output Power ($\mu\text{W}/\text{cm}^3$)	Resonance Frequency (Hz)	Resonance Frequency (Hz)	Output Power ($\mu\text{W}/\text{cm}^3$)	Resonance Frequency (Hz)	Output Power ($\mu\text{W}/\text{cm}^3$)	
Physical layout I	11	231	10.5	24	9.5	0.56	10	5.83			
	102	31.2	91	11.53	96.5	21.7	96.5	214.02			
	195.5	25	200.5	47	81	137	70.5	2140			
Physical layout IIIA	87	162.58	90	1103	36	909	33	13740			
					142	39	156.5	576.6			
	92	150.26	93	1609	34	778	20	15722			
Physical layout IIIB					187	19.64	208	470.5			

COMSOL Multiphysics models were built for each physical layout. Simulation values for Harvester 1 were close with all experiment values. For Harvester 2, since there was no given modulus of elasticity of the whole harvester, the modulus of elasticity was determined to match with experiment result. However, the modulus of elasticity value of Harvester 2 could not be matched to obtain the measured natural frequency for physical layout II. The output voltages of Harvester 2 for physical layout II and 3 were high (in the range of hundreds Volts). For these reasons, it is believed that the model for Harvester 2 did not fully describe the physics of this system.

For the range of loading resistors used, the oscilloscope and probe did not have loading effect on the harvester. With the tuning, Harvester 2 was able to retrieve energy at 60 Hz and produced a higher output power when both sources of energy were present. However, the output voltage was not a pure sinewave. This happened due to a slightly different in frequency. A theoretical output voltage was calculated and shown to be close to the measured output voltage. Maximum output power density recorded was 35.64 mW/cm^3 which is higher than all of the cantilever beam harvesters result presented in Chapter 2. This work was similar to Xu et al. which used magnets and wires to harvest EMF energy; however, the output density was approximately three times larger. This promising result exceeds the typical power density $200 \text{ } \mu\text{W/cm}^3$.

The amount of power estimated in a distribution power line was calculated. The output voltages under each source at higher displacement and current magnitude were estimated based on the fitted curve obtained by experiment measurement. The predicted voltage was the root mean square value of the sum of the voltage in each source. With maximum condition of 600 A current and 17.96 mm displacement, the predicted output

power was 14.18 mW when both source of energy were at 60 Hz frequency. It would need about 10 harvesters to produce enough power to supply the sensor with this prediction. It is important to ensure that the harvester material can be able to handle the amount of stress induce on it due to high amount of current and vibration in operating environment.

5.2 Possible Future Work

Although the results seem promising, the design of the harvester can still be optimized structure. The main goal of this project is to power a sensor that needs 130mW; however, this harvester can be used for other sensors. Possible expansion of the work could include:

- Implementing the harvester in real power line environment
- Stress analysis and prevention of high vibration magnitude and current techniques
- Further optimization design or design for smaller current for sensor used in buildings
- Investigation on number of harvesters needed for modular design
- Design of harvesting circuit or converter

BIBLIOGRAPHY

- [1] Z. L. Wang and W. Wu, "Nanotechnology-enabled energy harvesting for self-powered micro/nanosystems.," *Angew. Chem. Int. Ed. Engl.*, vol. 51, no. 47, pp. 11700–21, Nov. 2012.
- [2] L. Zuo and X. Tang, "Large-scale vibration energy harvesting," *J. Intell. Mater. Syst. Struct.*, vol. 24, no. 11, pp. 1405–1430, Jun. 2013.
- [3] M. A. Noras, S. P. Ramsey, and B. B. Rhoades "Projectile detection using quasi-electrostatic field sensor array," *Journal of Electrostatics*, vol. 71, no. 3, pp. 220- 223, 2013.
- [4] M. Vo and M. Noras, "Energy Harvesting from Electromagnetic Field Surrounding A Current Carrying Conductor," in *Proc. ESA Annual Meeting on Electrostatics*, 2013, pp. 1–12.
- [5] A. Khaligh, "Kinetic Energy Harvesting Using Piezoelectric and Electromagnetic Technologies—State of the Art," *IEEE Trans. Ind. Electron.*, vol. 57, no. 3, pp. 850–860, Mar. 2010.
- [5] F. Cottone, "Introduction to Vibration Energy Harvesting," 2011. [Online]. Available: [http://www.nipslab.org/files/file/nips summer school 2011/Cottone Introduction to vibration harvesting.pdf](http://www.nipslab.org/files/file/nips%20summer%20school%202011/Cottone%20Introduction%20to%20vibration%20harvesting.pdf). [Accessed: 13-Dec-2013].
- [6] J. A. Paradiso and T. Starner, "Energy Scavenging for Mobile and Wireless Electronics," *IEEE Pervasive Comput.*, vol. 4, no. 1, pp. 18–27, Jan. 2005.
- [7] H.-B. Fang, J.-Q. Liu, Z.-Y. Xu, L. Dong, L. Wang, D. Chen, B.-C. Cai, and Y. Liu, "Fabrication and performance of MEMS-based piezoelectric power generator for vibration energy harvesting," *Microelectronics J.*, vol. 37, no. 11, pp. 1280–1284, Nov. 2006.
- [8] H. a. Sodano, "Comparison of Piezoelectric Energy Harvesting Devices for Recharging Batteries," *J. Intell. Mater. Syst. Struct.*, vol. 16, no. 10, pp. 799–807, Oct. 2005.
- [9] H. a. Sodano, G. Park, and D. J. Inman, "Estimation of Electric Charge Output for Piezoelectric Energy Harvesting," *Strain*, vol. 40, no. 2, pp. 49–58, May 2004.
- [10] S. R. Anton and H. a. Sodano, "A review of power harvesting using piezoelectric materials (2003–2006)," *Smart Mater. Struct.*, vol. 16, no. 3, pp. R1–R21, Jun. 2007.
- [11] M. S. Vijaya, *Piezoelectric Materials and Devices Applications in Engineering*. CRC Press, 2013.

- [12] J. Colomer-farrarons, P. L. Miribel, E. Juanola, and J. Samitier, "Chapter 2: -Low-Power Energy Harvesting Solutions for Biomedical Devices," pp. 31–58.
- [13] L. Mateu, F. Moll, and U. Polit, "Review of Energy Harvesting Techniques and Applications for Microelectronics."
- [14] N. S. Shenck and J. A. Paradiso, "Energy scavenging with shoe-mounted piezoelectrics," *IEEE Micro*, vol. 21, no. 3, pp. 30–42, 2001.
- [15] S. E. From, "Scavenging Energy From Human Body : Design Of A," pp. 784–787, 2005.
- [16] J. J. Allen and A. J. Smits, "Energy Harvesting Eel," *J. Fluids Struct.*, vol. 15, no. 3–4, pp. 629–640, Apr. 2001.
- [17] V. H. Schmidt, "Piezoelectric energy conversion in windmills," *IEEE 1992 Ultrason. Symp. Proc.*, pp. 897–904, 1992.
- [18] S. Roundy, E. S. Leland, J. Baker, E. Carleton, E. Reilly, E. Lai, B. Otis, J. M. Rabaey, V. Sundararajan, and P. K. Wright, "Improving Power Output for Vibration-Based Energy Scavengers," *IEEE Pervasive Comput.*, vol. 4, no. 1, pp. 28–36, Jan. 2005.
- [19] Y. B. Jeon, R. Sood, J. -h. Jeong, and S.-G. Kim, "MEMS power generator with transverse mode thin film PZT," *Sensors Actuators A Phys.*, vol. 122, no. 1, pp. 16–22, Jul. 2005.
- [20] J. C. Park and J. Y. Park, "Asymmetric PZT bimorph cantilever for multi-dimensional ambient vibration harvesting," *Ceram. Int.*, vol. 39, pp. S653–S657, May 2013.
- [21] C. B. Williams and R. B. Yates, "Analysis of a micro-electric generator for microsystems," vol. 44, no. 0, 1995.
- [22] C. B. Williams, C. Shearwood, M. a. Harradine, P. H. Mellor, T. S. Birch, and R. B. Yates, "Development of an electromagnetic micro-generator," *IEE Proc. - Circuits, Devices Syst.*, vol. 148, no. 6, p. 337, 2001.
- [23] P. Pillatsch, E. M. Yeatman, and a S. Holmes, "Magnetic plucking of piezoelectric beams for frequency up-converting energy harvesters," *Smart Mater. Struct.*, vol. 23, no. 2, p. 025009, Feb. 2014.
- [24] E. Leland, R. White, and P. Wright, "Energy scavenging power sources for household electrical monitoring," *PowerMEMS* (Dec. 2006), pp. 165–168, 2006.

- [25] Q. R. Xu, R. Send, I. Paprotny, R. M. White, and P. K. Wright, "Miniature self-powered stick-on wireless sensor node for monitoring of overhead power lines," in 2013 IEEE Energy Conversion Congress and Exposition, 2013, pp. 2672–2675.
- [26] I. Paprotny, Q. Xu, W. W. Chan, R. M. White, and P. K. Wright, "Electromechanical Energy Scavenging From Current-Carrying Conductors," *IEEE Sens. J.*, vol. 13, no. 1, pp. 190–201, Jan. 2013.
- [27] W. He, P. Li, Y. Wen, J. Zhang, A. Yang, C. Lu, J. Yang, J. Wen, J. Qiu, Y. Zhu, and M. Yu, "Piezoelectric energy harvester scavenging AC magnetic field energy from electric power lines," *Sensors Actuators A Phys.*, vol. 193, pp. 59–68, Apr. 2013.
- [28] Y. Uzun and E. Kurt, "The effect of periodic magnetic force on a piezoelectric energy harvester," *Sensors and Actuators A : Physical*, vol. 192, pp. 58–68, 2013.
- [29] M. Ferrari, M. Baù, M. Guizzetti, and V. Ferrari, "A single-magnet nonlinear piezoelectric converter for enhanced energy harvesting from random vibrations," *Sensors Actuators A Phys.*, vol. 172, no. 1, pp. 287–292, 2011.
- [30] K. Fan, J. Chang, F. Chao, and W. Pedrycz, "Design and development of a multipurpose piezoelectric energy harvester," *Energy Convers. Manag.*, vol. 96, pp. 430–439, 2015.
- [31] V. R. Challa, M. G. Prasad, and F. T. Fisher, "A coupled piezoelectric–electromagnetic energy harvesting technique for achieving increased power output through damping matching," *Smart Mater. Struct.*, vol. 18, no. 9, p. 095029, 2009.
- [32] S. G. Kelly, "Fundamentals of Mechanical Vibrations." McGraw-Hill, Inc, Highston NJ, 1993.
- [33] N. O. Myklestad, "Vibration Analysis" McGraw-Hill, NY, 1956.
- [34] "Thermal expansion and the bi-material strip." University of Cambridge 2004. [Online]. Available: <http://www.doitpoms.ac.uk/tlplib/thermal-expansion/printall.php>
- [35] "Natural Frequencies for Common Systems." University of Massachusetts Lowell. Pg 1-6. [Online]. Available: http://faculty.uml.edu/pavitabile/22.403/web_downloads/Frequencies_of_Common_Systems.PDF
- [36] Takuro Ikeda, "Fundamentals of Piezoelectricity." Oxford University Press. Oxford, NY, Tokyo, 1990.
- [37] I. American Piezo, "Physical and piezoelectric properties of apc materials," Online, 2012. [Online]. Available: <http://www.americanpiezo.com/apcmaterials/piezoelectric-properties.html>

- [38] J. Baker, "Alternative Geometries for Increasing Power Density in Vibration Energy Scavenging," in 3rd International Energy Conversion Engineering Conference 15 - 18 August 2005, San Francisco, California, 2005, no. August, pp. 1–12.
- [39] "Magnetic Fields and Magnetic Field Lines." OpenStax Connexion. 2009.[Online] Available: <http://cnx.org/content/m42370/latest/?collection=col11406/latest>
- [40] "Bar Magnet." Department of Physic and Astronomy at Georgia State University 2012. [Online]. Available: <http://hyperphysics.phy-astr.gsu.edu/hbase/magnetic/elemag.html>
- [40] L. Dhakar, H. Liu, F. E. H. Tay, and C. Lee, "A new energy harvester design for high power output at low frequencies," *Sensors Actuators A Phys.*, vol. 199, pp. 344–352, Sep. 2013.
- [42] P. E. Harvesters, "Piezoelectric Energy Harvesters," pp. 1–24.
- [43] P. Layers, "Vulture Products - Material Properties FR4."
- [44] T. Irvine, "Welcome to Vibration data," *Newsletter*, no. May, pp. 1–17, 2005.
- [45] "Fundamentals of Distribution Systems," in *Electric Power Distribution Handbook*, CRC Press, 2003.

APPENDIX A: SOURCES COMBINATION THEORETICAL CALCULATION
MATLAB CODE

```
%11-5-2015
%Energy Harvesting Master Project
home;
clear all;
%Theoretical Combination of Source Calculation
%Input from Measured Results under EMF only
v1=20.5/.707;
v2=26.7/.707;
v3=29.7/.707;
%Input from Measured Results under Mechanical Vibration only
m1=15.1/.707
f1=61.3;%Assumed the frequency different was about 0.3 between the two
sources
f2=61;
%Sum of voltage under each separate source
t=0:1/10^3:1;
c1=v1*sin(2*pi*f1*t)+m1*sin(2*pi*t*f2);
c2=v2*sin(2*pi*f1*t)+m1*sin(2*pi*t*f2);
c3=v3*sin(2*pi*f1*t)+m1*sin(2*pi*t*f2);
%Calculate RMS value
a=rms(c1)
a1=rms(c2)
a2=rms(c3)
```

APPENDIX A: OUTPUT POWER PREDICTION ON OPERATING ENVIROMENT MATLAB CODE

```

%11-17-2015
%Energy Harvesting Master Project
%Prediction on Operating Environment
%Loading Experiment Data
data=xlsread('60Hz Results-10-30-15.xlsx','Fitting');
Displacement=data(:,1);
Voltage=data(:,2);
curr=data(:,3);
V_emf=data(:,4);
%cftool %Run the Curve Fitting Tool

%Prediction of output power under power line environment
%Assume a conductor of 500kcmil used
%Fitting for Mechanical Vibrations
a =15.35;
b =0.3204;
c =-4.615;
fmech=150;
t=0:1/10^3:1;

%Generating Output Voltage Graph for Mechanical Vibration
Aeolian_factor=1;%[0.01 1]0.1832
disp=17.96*Aeolian_factor % unit mm
Vmech = a*disp^b+c %unit Vrms

%Fitting for EMF
current=0.707*100;%527
a1 =-404.5;
b1 =-0.8146;
c1 =44.16;
Vemf = a1*current^b1+c1

%Prediction
combine=Vmech./0.707.*sin(2.*pi.*60.*t)+Vemf/0.707.*sin(2.*pi.*fmech.*t
);
comb=rms(combine)

```